SOURCE DATA · TRANSPARENT PROCESS · OPEN ACCESS · CHECK FOR UPDATES

NT-3 contributes to chemotherapy-induced neuropathic pain through TrkC-mediated CCL2 elevation in DRG neurons

Dilip Sharma[1], Xiaozhou Feng[1], Bing Wang[1], Bushra Yasin [1], Alex Bekker[1], Huijuan Hu [1,2] & Yuan-Xiang Tao [1,2,3 ✉]

Abstract

Cancer patients undergoing treatment with antineoplastic drugs often experience chemotherapy-induced neuropathic pain (CINP), and the therapeutic options for managing CINP are limited. Here, we show that systemic paclitaxel administration upregulates the expression of neurotrophin-3 (*Nt3*) mRNA and NT3 protein in the neurons of dorsal root ganglia (DRG), but not in the spinal cord. Blocking NT3 upregulation attenuates paclitaxel-induced mechanical, heat, and cold nociceptive hypersensitivities and spontaneous pain without altering acute pain and locomotor activity in male and female mice. Conversely, mimicking this increase produces enhanced responses to mechanical, heat, and cold stimuli and spontaneous pain in naive male and female mice. Mechanistically, NT3 triggers tropomyosin receptor kinase C (TrkC) activation and participates in the paclitaxel-induced increases of C–C chemokine ligand 2 (*Ccl2*) mRNA and CCL2 protein in the DRG. Given that CCL2 is an endogenous initiator of CINP and that Nt3 mRNA co-expresses with TrkC and *Ccl2* mRNAs in DRG neurons, NT3 likely contributes to CINP through TrkC-mediated activation of the Ccl2 gene in DRG neurons. NT3 may be thus a potential target for CINP treatment.

Introduction

Chemotherapy-induced neuropathic pain (CINP) is one of the side effects caused by chemotherapeutic drugs during cancer treatments (Grisold et al, 2012; Windebank and Grisold, 2008). Although the incidence and severity of CINP are correlated with the duration and dose of chemotherapy drugs, many cancer patients eventually discontinue cancer therapy due to CINP and have the reduced survival rates (Argyriou et al, 2012; Grisold et al, 2012). Current treatments of CINP are highly limited in part due to the elusive mechanisms underlying this disorder. Chemotherapy drugs have unrestricted access to dorsal root ganglion (DRG) due to the lack of an effective vascular permeability barrier (Devor, 1999; Jimenez-Andrade et al, 2008). These drugs led to ectopic discharge, which is considered as a CINP trigger, in DRG neurons (Li et al, 2017a, 2018; Sisignano et al, 2016; Zhang and Dougherty, 2014). The ectopic discharge may be associated with the changes in pain-related genes induced by chemotherapy drugs at both transcriptional and translational levels in DRG (Ito et al, 2017; Li et al, 2014, 2017a, 2018; Makker et al, 2017; Mao et al, 2017, 2019; Nie et al, 2018; Sisignano et al, 2016; Yilmaz and Gold, 2015; Zhang et al, 2013; Zhang and Dougherty, 2014). For example, C–C chemokine ligand 2 (CCL2, also called as MCP-1) directly excited DRG neurons through activation of its C–C motif receptor 2 (CCR2) by autocrine or paracrine processes (Jung et al, 2008; Sun et al, 2006; Van Steenwinckel et al, 2011). CCR2 activation sensitized nociceptors via transactivation of transient receptor potential channels (Jung et al, 2008). Systemic administration of the chemotherapy drugs, paclitaxel and oxaliplatin, upregulated the expression of CCL2 in the DRG neurons (Al-Mazidi et al, 2018; Curry et al, 2018; Illias et al, 2018; Wen et al, 2023; Zhang et al, 2016a). Genetic knockdown or pharmacological inhibition of DRG CCL2 alleviated these drugs-induced nociceptive hypersensitivities (Al-Mazidi et al, 2018; Curry et al, 2018; Illias et al, 2018; Zhang et al, 2016a). CCL2 is likely an endogenous initiator of CINP. Understanding the mechanisms by which chemotherapy drugs cause the changes of these pain-associated genes (such as CCL2) are critical for developing a new avenue for CINP management.

Neurotrophin-3 (NT3), a member of the nerve growth factor family of neurotrophins (Richner et al, 2014), binds with high affinity to its specific receptor, tropomyosin receptor kinase C (TrkC), and less strongly to the p75 non-tyrosine receptor (NTR) (Richner et al, 2014). NT3 is an important regulator of neuronal functions, survival, growth, differentiation, cell fate choices, neurite morphology, and cell death (Mendell et al, 1999). Peripheral nerve injury increases the expression of NT3 and TrkC in the neurons of

[1]Department of Anesthesiology, New Jersey Medical School, Rutgers, The State University of New Jersey, Newark, NJ 07103, USA. [2]Department of Physiology, Pharmacology & Neuroscience, New Jersey Medical School, Rutgers, The State University of New Jersey, Newark, NJ 07103, USA. [3]Department of Cell Biology & Molecular Medicine, New Jersey Medical School, Rutgers, The State University of New Jersey, Newark, NJ 07103, USA. ✉E-mail: yuanxiang.tao@njms.rutgers.edu

the DRG (Kazemi et al, 2017; Tender et al, 2011; Wang et al, 2008). They were also upregulated in the DRG, sciatic nerve, and skin nerves under the conditions of rat and human diabetic neuropathy (Cai et al, 1999; Kennedy et al, 1998; Shimoshige et al, 2010; Terenghi et al, 1997). Intrathecal NT3 or NT3 directly delivered into DRG produced mechanical allodynia in normal rats (White, 1998; Zhou et al, 2000). Intrathecal NT3 antisense oligonucleotide or local and systemic NT3 antiserum attenuated nerve injury-induced mechanical allodynia (Deng et al, 2000; Quintao et al, 2008; White, 2000; Zhou et al, 2000). In contrast, early studies from one group reported that intrathecal NT3 inhibited nerve injury-induced thermal hyperalgesia (Wilson-Gerwing et al, 2005, 2008; Wilson-Gerwing and Verge, 2006). It appears that the role of NT3 in nerve trauma-induced neuropathic pain is still elusive. The expression and function of NT3 in the DRG under the conditions of CINP are unknown.

In this study, we first observed whether systemic injection of the chemotherapy drug paclitaxel altered NT3 expression and distribution in the DRG. We then investigated whether this alternation was required and sufficient for the paclitaxel-induced CINP. Finally, we explored the mechanism through which this alteration contributed to paclitaxel-induced CINP.

Results

NT3 expression is increased in the DRGs after systemic paclitaxel injection

To demonstrate the role of NT3 in CINP, we first examined NT3 abundance in two pain-related regions, DRG and spinal cord, from CD1 mice after systemic administration of paclitaxel. Consistent with our previous studies (Mao et al, 2019; Yang et al, 2021), intraperitoneal (i.p.) injection of paclitaxel, not vehicle, produced robust and long-lasting mechanical allodynia evidenced by marked increases in paw withdrawal frequencies in response to 0.07 g and 0.4 g von Frey filaments on both left (Fig. 1A,B) and right sides. This nociceptive hypersensitivity occurred on day 7 after the first paclitaxel injection and persisted for at least 14 days (Fig. 1A,B). Correlating with these behavioral changes, the expression of NT3 was time-dependently upregulated in the DRGs after paclitaxel injection. The amount of $Nt3$ mRNA expression in the L3/4 DRGs was increased by 1.4-fold ($P > 0.05$), 1.8-fold ($P < 0.05$), 2.1-fold ($P < 0.01$), and 1.8-fold ($P < 0.05$) on days 7, 10, 14, and 21, respectively, after the first paclitaxel injection as compared to the corresponding vehicle-treated mice (Fig. 1C). Consistently, the level of NT3 protein in the L3/4 DRGs was elevated by 1.4-fold ($P < 0.05$), 1.5-fold ($P < 0.05$), 2.2-fold ($P < 0.01$), and 1.4-fold ($P < 0.05$) on days 7, 10, 14, and 21 after the first paclitaxel injection, respectively, as compared to the corresponding vehicle-treated mice (0 day; Fig. 1D). As expected, i.p. injection of vehicle did not change basal levels of $Nt3$ mRNA and its coding protein in the L3/4 DRGs during the observation period (Fig. 1C,D). The amount of NT3 protein was not altered in the L3/4 spinal cord during the observation period after the first paclitaxel injection (Fig. 1E).

The distribution pattern of NT3 in the DRGs of CD1 mice was examined after systemic injection of paclitaxel. $Nt3$ mRNA was expressed in cellular cytoplasm and co-localized with β-tubulin III (a specific neuronal marker) but not with glutamine synthetase (GS, a marker for satellite glial cells), in DRG cells of paclitaxel- or vehicle-injected mice (Fig. 2A,B), indicating that $Nt3$ mRNA expresses exclusively in DRG neurons. Approximately 5.5% and 29.6% of β-tubulin III-labeled DRG neurons were positive for $Nt3$ mRNA in the vehicle and paclitaxel mice, respectively, on day 14 after the first paclitaxel or vehicle injection (Fig. 2A). A cross-sectional area analysis of neuronal somata showed that about 25% of $Nt3$ mRNA-labeled neurons were small (<500 μm² in the area), 36% for medium (500–1000 μm² in the area), and 39% for large (>1000 μm² in the area) in the DRGs of the paclitaxel-treated mice (Fig. 2C). Consistently, about 30% of $Nt3$ mRNA-labeled neurons were positive for CGRP (a marker for small DRG peptidergic neurons; Fig. 2D,H), 34% for NF200 (a marker for medium/large neurons and myelinated Aβ fibers; Fig. 2E,H), 33% for IB4 (a marker for small nonpeptidergic neurons; Fig. 2F,H) and 18% for tyrosine hydroxylase (TH, a marker for small low-threshold neurons; Fig. 2G,H) in the paclitaxel-treated DRGs.

Taken together, the neuronal distribution pattern of $Nt3$ mRNA and paclitaxel-induced increases of $Nt3$ mRNA and protein in the DRGs suggests NT3 involvement in paclitaxel-induced CINP.

Effect of blocking DRG NT3 upregulation on paclitaxel-induced nociceptive hypersensitivities

To examine whether DRG NT3 upregulation participated in the paclitaxel-induced CINP, we first blocked DRG NT3 upregulation through a single microinjection of $Nt3$ short interfering RNA (NT3 siRNA; dissolved in PBS) into unilateral L3/4 DRGs of adult CD1 male mice 7 days after the first i.p. injection of vehicle or paclitaxel. Negative control scrambled siRNA (NC siRNA; dissolved in PBS) was used as a control. As expected, the level of NT3 was increased by 1.7-fold ($P < 0.01$) in the microinjected L3/4 DRGs from paclitaxel plus NC siRNA-treated group compared to that in vehicle plus NC siRNA-treated group, 14 days after the first paclitaxel injection (Fig. 3A). This increase was not seen in the paclitaxel plus NT3 siRNA-treated group (Fig. 3A). Basal levels of NT3 were not significantly changed in the microinjected L3/4 DRGs of the NT3 siRNA plus vehicle-treated group (Fig. 3A). Paclitaxel injection produced mechanical allodynia in response to mechanical stimuli (0.07 g and 0.4 g von Frey filaments) and heat and cold hyperalgesia in response to heat and cold stimuli starting day 7 after the first paclitaxel injection and persisting for at least 7 days in NC siRNA-microinjected mice (Fig. 3B–H). These nociceptive hypersensitivities were significantly alleviated on the ipsilateral (not contralateral) side in the paclitaxel plus NT3 siRNA-treated group on days 10, 12, and 14 post the first paclitaxel injection (Fig. 3B–H). Neither NT3 siRNA microinjection nor NC siRNA microinjection altered basal paw withdrawal responses on either side in the vehicle-treated group (Fig. 3B–H).

Neuronal hyperexcitability in the DRGs caused by systemic administration of paclitaxel triggers the hyperactivation of neurons and astrocytes in the spinal cord dorsal horn likely through augmenting the release of neurotransmitters and/or neuromodulators in primary afferents (Wen et al, 2023; Yang et al, 2021). To further confirm our behavioral observations above, we examined whether DRG microinjection of NT3 siRNA also affected the hyperactivities of spinal cord dorsal horn neurons and astrocytes, as documented by increases in the levels of phosphorylated
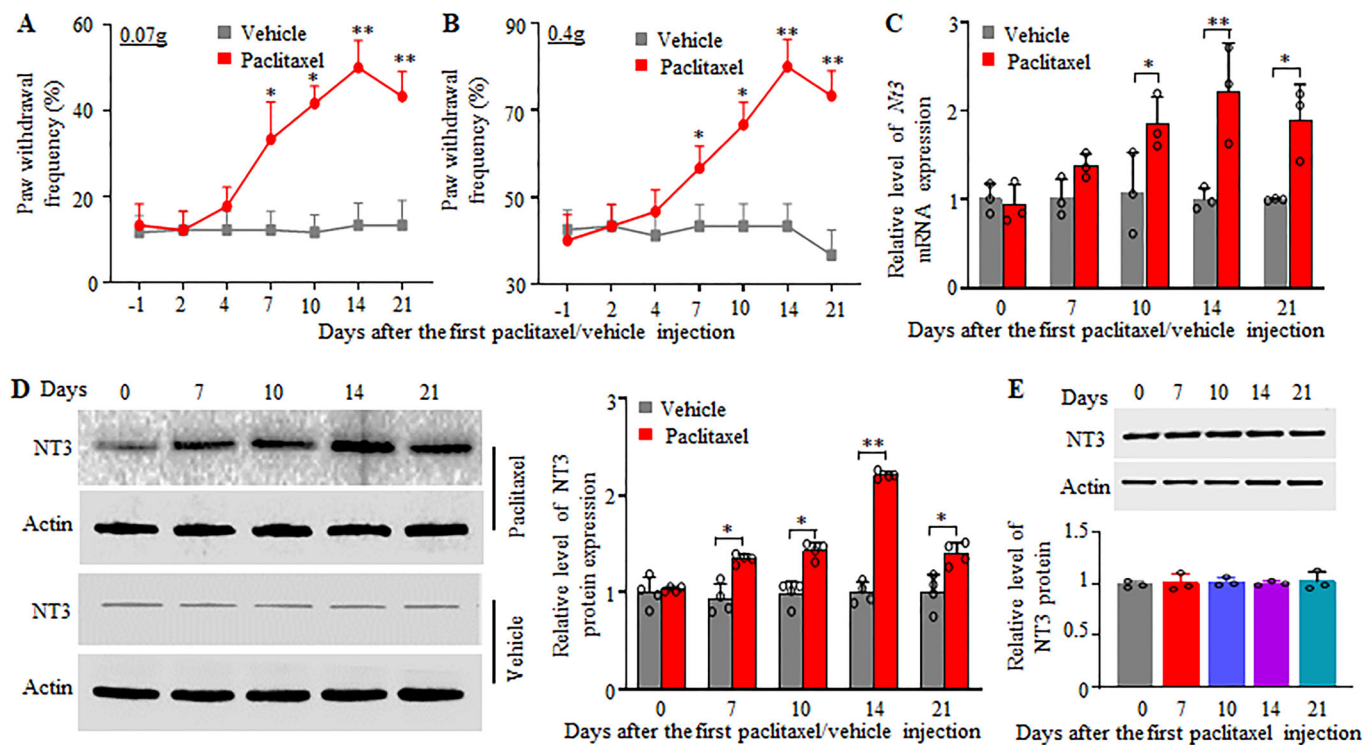
Figure 1. NT3 abundance is increased in the DRG after paclitaxel injection.

Data: mean ± SD. (A, B) Intraperitoneal injection of paclitaxel produced mechanical allodynia as evidenced by the increases in paw withdrawal frequencies in response to 0.07 g (A) and 0.4 g (B) von Frey filaments on the left side. $n = 12$ mice/time point. $*P < 0.05$, $**P < 0.01$ versus the vehicle-treated group at the corresponding time points by two-way ANOVA with repeated measures followed by post hoc Tukey test. (C, D) The levels of $Nt3$ mRNA (C) and NT3 protein (D) in L3/4 DRGs on different days as indicated after the first injection of paclitaxel or vehicle. D: representative Western blots (left) and a summary of the densitometric analysis (right) are shown. $n = 3$ biological repeats (3 mice)/time point. $*P < 0.05$, $**P < 0.01$ by two-way ANOVA followed by post hoc Tukey test. (E) The amount of NT3 protein in the L3/4 spinal cord on different days as indicated after the first injection of paclitaxel. $n = 3$ biological repeated (3 mice)/time point. $P > 0.05$ by one-way ANOVA followed by post hoc Tukey test. Source data are available online for this figure.

extracellular signal-regulated kinase ½ (p-ERK1/2, a marker for neuronal hyperactivation) and glial fibrillary acidic protein (GFAP, a marker for astrocyte hyperactivation), respectively. The levels of p-ERK1, p-ERK2 and GFAP were increased by 3.0 ($P < 0.01$)-, 3.1 ($P < 0.01$)-, and 2.1 ($P < 0.05$)-fold, respectively, in the ipsilateral L3/4 dorsal horn of the paclitaxel plus NC siRNA-treated group, as compared to those in vehicle plus NC siRNA-treated group on day 14 post the first paclitaxel or vehicle injection (Fig. 3I). These increases were not observed in the paclitaxel plus NT3 siRNA-treated mice (Fig. 3I). No significant differences in basal amounts of total ERK1/2 were seen in the ipsilateral L3/4 dorsal horn among all treated groups (Fig. 3I). Neither siRNA affected basal levels of p-ERK1/2, ERK1/2 and GFAP in the ipsilateral L3/4 dorsal horn in the vehicle-treated group (Fig. 3I).

Similar findings were observed in the paclitaxel- or vehicle-treated female mice with DRG microinjection of NT3 siRNA or NC siRNA (Fig. 4A–I).

To exclude the possibilities that the observed behavioral changes above may be caused by siRNA off-targets and/or microinjection-induced tissue damage, we carried out i.p. injection of paclitaxel or vehicle 7 days before i.p. injection of tamoxifen (1 mg/mouse daily for 7 consecutive days; dissolved in 90% of sunflower seed oil and 10% of dimethyl sulfoxide) in male NT3$^{f/f}$ mice and NT3 cKD mice. As expected, the levels of $Nt3$ mRNA and NT3 proteins were

increased by 2.7- and 2.5-fold, respectively, in the bilateral L3/4 DRGs from the paclitaxel plus tamoxifen-treated NT3$^{f/f}$ mice, as compared to those in the vehicle plus tamoxifen-treated NT3$^{f/f}$ mice on day 28 post the first paclitaxel injection (Fig. 5A,B). These increases were significantly blocked in the paclitaxel plus tamoxifen-treated NT3 cKD mice (Fig. 5A,B). Basal levels of $Nt3$ mRNA and NT3 proteins were not altered in the bilateral L3/4 DRGs from the vehicle plus tamoxifen-treated NT3 cKD mice (Fig. 5A,B). Blocking the paclitaxel-induced increase of NT3 in the bilateral L3/4 DRGs of male NT3 cKD mice following tamoxifen injection impaired the paclitaxel-induced mechanical allodynia and heat and cold hyperalgesia on both left and right sides from day 12 to day 28 post the first paclitaxel injection (Fig. 5C–I). These NT3 cKD mice with tamoxifen injection failed to exhibit significant preference toward either the saline- or lidocaine-paired chamber on day 21 post the first paclitaxel injection, indicating the reduction in the paclitaxel-induced stimulation-independent spontaneous ongoing pain (Fig. 5J,K). As expected, the paclitaxel-evoked increases of neuronal/astrocyte hyperactivities in the L3/4 dorsal horn from the tamoxifen-injected NT3$^{f/f}$ mice were not detected in the tamoxifen-injected NT3 cKD mice on day 28 following the first paclitaxel injection (Fig. 5L). After vehicle injection, basal paw withdrawal responses on the bilateral sides of the tamoxifen-treated NT3$^{f/f}$ mice and NT3 cKD mice were not changed during the
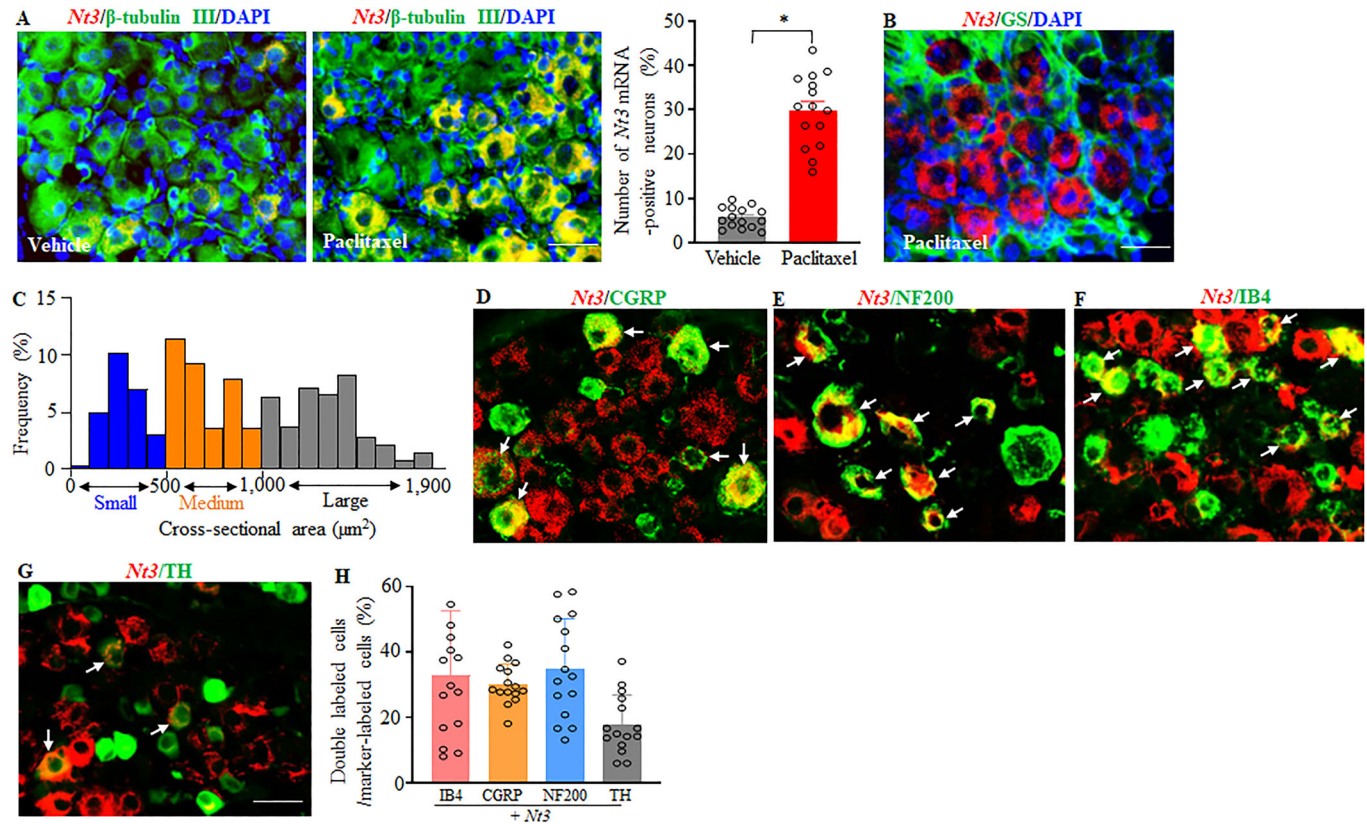
Figure 2. Distribution of *Nt3* mRNA in the DRG from the vehicle- or paclitaxel-treated mice.

Data: mean ± SD. (**A, B**) Representative images of in situ hybridization histochemistry (ISHH) for *Nt3* mRNA (red) and immunohistochemistry for β-tubulin III (green; **A**) or glutamine synthetase (GS; green; **B**) in the L3/4 DRGs 14 days after the first paclitaxel or vehicle injection. Cellular nuclei were labeled by 4′, 6-diamidino-2- phenylindole (DAPI; blue). $n = 9$–12 sections from three mice/group. *$P < 0.05$ by two-tailed unpaired Student t test. Scale bars: 50 µm. (**C**) Size distribution of *Nt3* mRNA-labeled neuronal somata in the L3/4 DRGs 14 days after the first paclitaxel injection. Small, 25%, medium, 36%; large, 39%. (**D–H**) Representative images of ISHH for *Nt3* mRNA (red) and immunohistochemistry for different DRG cell markers (calcitonin gene-related peptide (CGRP; green; **D**), neurofilament 200 (NF200; green; **E**), isolectin B4 (IB4; green; **F**), or tyrosine hydroxylase (TH; green; **G**)) in the L3/4 DRGs 14 days after the first paclitaxel injection. Arrows: double-labeling neurons. Statistical summary of number of double-labeling neurons (**H**). $n = 9$–12 sections from three mice. Scale bar: 50 µm. Source data are available online for this figure.

---

observation periods (Fig. 5C–I). All siRNA-microinjected male and female mice and tamoxifen-treated NT3$^{f/f}$ male mice or NT3 cKD male mice exhibited normal locomotor activity (Table EV1).

Mimicking the paclitaxel-induced DRG NT3 upregulation produces nociceptive hypersensitivities in naive mice

We next inquired whether the paclitaxel-induced DRG NT3 upregulation was sufficient for CINP. To this end, we mimicked the paclitaxel-indued DRG NR3 increase through microinjection of AAV5 expressing full-length *Nt3* mRNA (AAV5-NT3) into unilateral L3/4 DRGs of naive male CD1 mice. AAV5 expressing green fluorescent protein (AAV5-GFP) was used as a control. As anticipated, the levels of *Nt3* mRNA and NT3 protein in the ipsilateral L3/4 DRGs were increased by 3.4- and 2.2-fold, respectively, in mice microinjected with AAV5-NT3 compared to those microinjected with AAV5-GFP 8 weeks after viral micro-injection (Fig. 6A,B). More interestingly, DRG microinjection of AAV5-NT3, but not AAV5-GFP, produced significant increases in paw withdrawal frequencies in response to 0.07 g and 0.4 g von Frey

filament stimuli and decreases in paw withdrawal latencies in response to heat and cold stimuli on the ipsilateral (not contralateral) side (Fig. 6C–F). These nociceptive hypersensitivities developed 4 weeks post-viral microinjection and persisted for at least 4 weeks (Fig. 6C–F). This microinjection also led to stimulation-independent spontaneous pain and increased neuronal and astrocyte activities in the ipsilateral L3/4 dorsal horn 8 weeks after viral microinjection (Fig. 6G–I). Neither viral microinjection affected locomotor functions (Table EV1). Similar observations were found in naive female mice after DRG microinjection of AAV5-NT3 or AAV5-GFP (Fig. 7A–I; Table EV1). Together, these findings indicate that mimicking the paclitaxel-induced DRG NT3 increase produces both spontaneous and evoked nociceptive hypersensitivities in naive male and female mice.

TrkC, but not p75 receptor, mediates the NT3-induced nociceptive hypersensitivity

We further determined how DRG upregulated NT3 caused nociceptive hypersensitivities. The biological effects of NT3 are
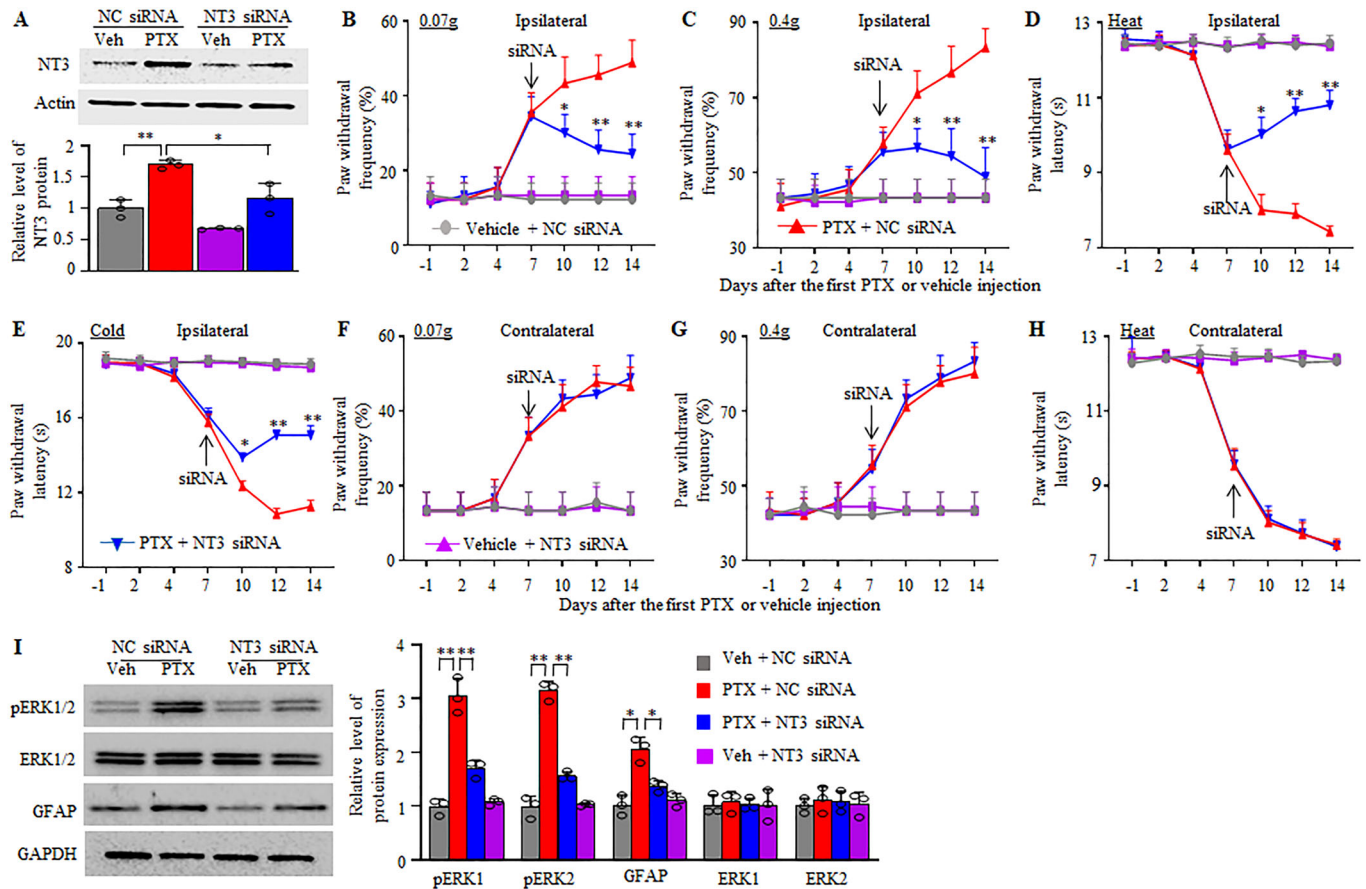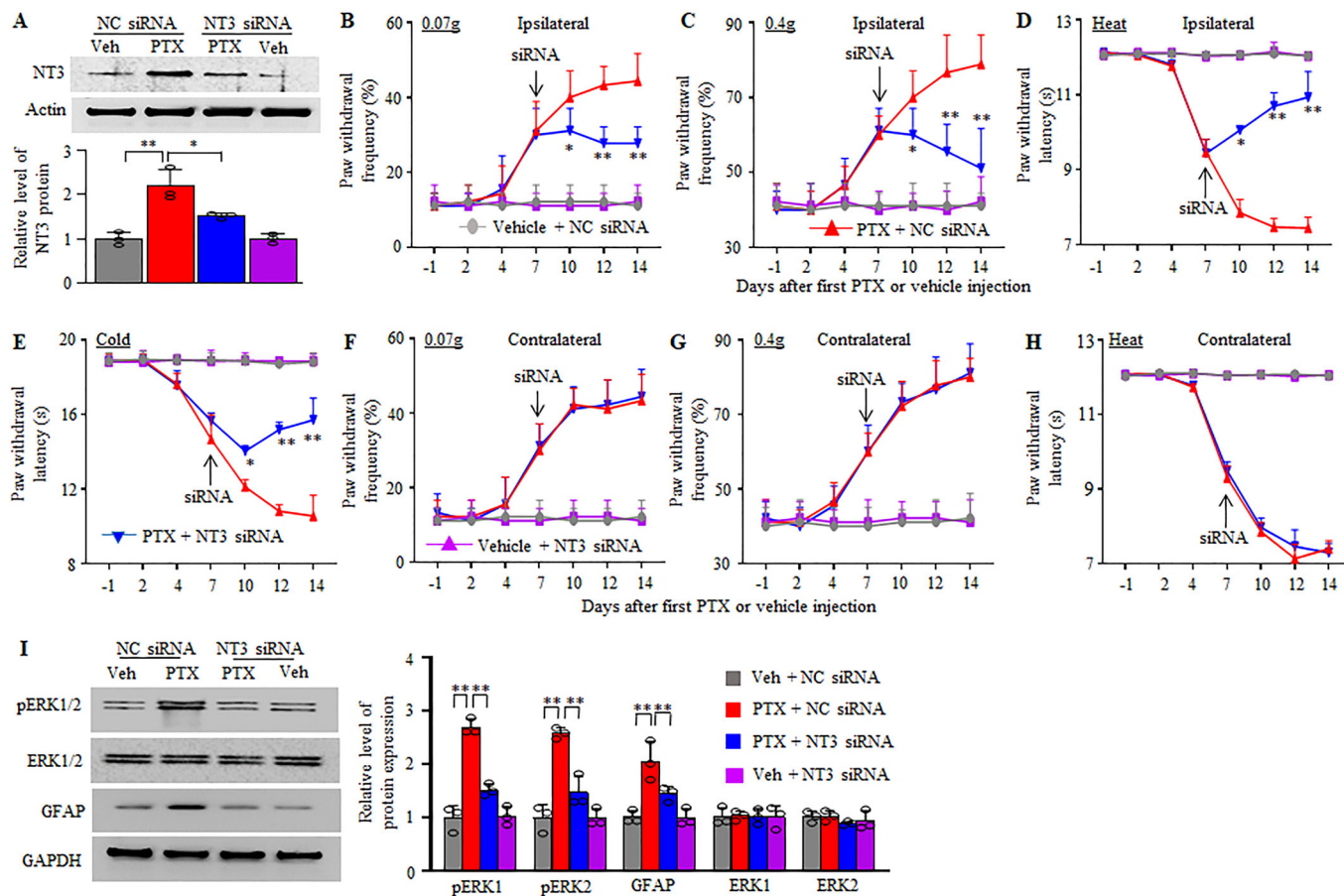
Figure 3. Effect of microinjection of NT3 siRNA or negative control scrambled siRNA (NC siRNA) into unilateral L3/4 DRGs on paclitaxel-induced nociceptive hypersensitivity in male mice.

Data: mean ± SD. (A) Expression of NT3 protein in the ipsilateral L3/4 DRGs 14 days after the first injection of paclitaxel (PTX) or vehicle (Veh) from the NT3 siRNA- or NC siRNA-microinjected male mice. $n = 3$ biological repeats (6 mice)/group. $*P < 0.05$, $**P < 0.01$ by two-way ANOVA followed by post hoc Tukey test. (B–H) Paw withdrawal frequency to 0.07 g (B, F) and 0.4 g (C, G) von Frey filament stimuli and paw withdrawal latency to heat (D, H) and cold (E) stimuli on the ipsilateral (B–E) and contralateral (F–H) side on days as indicated from male mice with DRG microinjection of NT3 siRNA or NC siRNA 7 days after the first injection of paclitaxel (PTX) or vehicle. $n = 9$ mice/group. $*P < 0.05$, $**P < 0.01$ versus the paclitaxel plus NC siRNA-treated group at the corresponding time points by three-way ANOVA with repeated measures followed by post hoc Tukey test. (I) Levels of p-ERK1/2, total ERK1/2, and GFAP in the ipsilateral L3/4 dorsal horn 14 days after the first injection of paclitaxel (PTX) or vehicle (Veh) from male mice with DRG microinjection of NT3 siRNA or NC siRNA. $n = 3$ mice/group. $*P < 0.05$, $**P < 0.01$ by two-way ANOVA followed by Tukey post hoc test. Source data are available online for this figure.

produced via NT3 binding to TrkC and p75NTR (Richner et al, 2014). We examined whether DRG TrkC and p75NTR knockdown through microinjection of specific TrkC siRNA and p75NTR siRNA, respectively, into the ipsilateral L3/4 DRGs 35 days after AAV5-NT3 microinjection into unilateral L3/4 DRGs on nociceptive hypersensitivities in naive CD1 male mice. As expected, basal levels of *Nt3* mRNA/protein were significantly increased in the ipsilateral L3/4 DRGs from the AAV5-NT3 (not AAV5-GFP) plus control scrambled siRNA-, TrkC siRNA-, or p75NTR siRNA-treated groups (Fig. 8A,B), whereas basal levels of *TrkC* mRNA/protein and *p75 NTR* mRNA/protein were markedly decreased in the ipsilateral L3/4 DRGs from the TrkC siRNA plus AAV5-GFP- or AAV5-NT3-treated groups and from the p75NTR siRNA plus AAV5-GFP or AAV5-NT3, respectively, on day 42 after AAV5 microinjection (Fig. 8A,B). More importantly, the increases in paw withdrawal frequencies to 0.07 g and 0.4 g von Frey filament stimuli and decreases in paw withdrawal latencies to heat and cold stimuli

on the ipsilateral side in the AAV5-NT3 plus control scrambled siRNA-treated group were impaired in the AAV5-NT3 plus TrkC siRNA-treated group, but not in the AAV5-NT3 plus p75NTR siRNA-treated group (Fig. 8C–F). None of these siRNAs altered basal responses to mechanical, heat and cold stimuli on the contralateral side of the AAV5-NT3-treated group and on both sides of the AAV5-GFP-treated group (Fig. 8C–I). In addition, significant increases in the levels of p-ERK1/2 and GFAP in the ipsilateral L3/4 dorsal horn on day 42 post-DRG AAV5-NT3 microinjection in the control scrambled siRNA-treated group were found in the p75NTR siRNA-treated group, but not in the TrkC siRNA-treated group (Fig. 8J). No alternations in basal amounts of total ERK1/2 in the ipsilateral L3/4 dorsal horn (Fig. 8J) and locomotor functions (Table EV1) were seen among siRNA-treated groups. These findings suggest that NT3 produces nociceptive hypersensitivity primarily through the activation of TrkC, but not p75NTR, in the DRG neurons.

Figure 4. Effect of microinjection of NT3 siRNA or negative control scrambled siRNA (NC siRNA) into unilateral L3/4 DRGs on paclitaxel-induced nociceptive hypersensitivity in female mice.

Data: mean ± SD. (A) Expression of NT3 protein in the ipsilateral L3/4 DRGs 14 days after the first injection of paclitaxel (PTX) or vehicle (Veh) from the NT3 siRNA- or NC siRNA-microinjected female mice. $n = 3$ biological repeats (6 mice)/group. *$P < 0.05$, **$P < 0.01$ by two-way ANOVA followed by post hoc Tukey test. (B–H) Paw withdrawal frequency to 0.07 g (B, F) and 0.4 g (C, G) von Frey filament stimuli and paw withdrawal latency to heat (D, H) and cold (E) stimuli on the ipsilateral (B–E) and contralateral (F–H) side on the days as indicated from female mice with DRG microinjection of NT3 siRNA or NC siRNA on day 7 after the first injection of paclitaxel or vehicle. $n = 9$ mice/group. *$P < 0.05$, **$P < 0.01$ versus the paclitaxel plus NC siRNA-treated group at the corresponding time points by three-way ANOVA with repeated measures followed by post hoc Tukey test. (I) Levels of p-ERK1/2, total ERK1/2, and GFAP in the ipsilateral L3/4 dorsal horn 14 days after the first injection of paclitaxel (PTX) or vehicle (Veh) from female mice with DRG microinjection of NT3 siRNA or NC siRNA. $n = 3$ mice/group. **$P < 0.01$ by two-way ANOVA followed by Tukey post hoc test. Source data are available online for this figure.

Upregulated NT3 is responsible for the TrkC-mediated CCL2 increase in the paclitaxel-exposed DRG

Finally, we elucidated the mechanism by which DRG upregulated NT3 contributed to the paclitaxel-induced CINP. The chemokine CCL2 (also called as MCP-1) plays a pivotal role in CINP (Al-Mazidi et al, 2018; Curry et al, 2018; Illias et al, 2018; Wen et al, 2023; Zhang et al, 2016b). Given that CCL2 was a potential downstream target of NT3/TrkC (Salvador et al, 2014), we predicted that CCL2 might mediate the role of DRG upregulated NT3 in the paclitaxel-induced CINP. Consistent with previous reports (Al-Mazidi et al, 2018; Curry et al, 2018; Illias et al, 2018; Wen et al, 2023; Zhang et al, 2016b), the level of CCL2 was substantially increased in the bilateral L3/4 DRGs on day 14 after the first paclitaxel injection from the NC siRNA-treated male (Fig. 9A) and female (Fig. 9B) CD1 mice or on day 28 after the first paclitaxel injection from the tamoxifen-treated NT3[f/f] male mice

(Fig. 9C). These increases were significantly blocked in the paclitaxel plus NT3 siRNA-treated CD1 male (Fig. 9A) and female (Fig. 9B) mice or in the paclitaxel plus tamoxifen-treated NT3 cKD male mice (Fig. 9C). There was also a significant increase in level of TrkC in the ipsilateral L3/4 DRG on day 14 after the first paclitaxel injection from the NC siRNA-treated male (Fig. 9A) and female (Fig. 9B) CD1 mice or on day 28 after the first paclitaxel injection from the tamoxifen-treated NT3[f/f] male mice (Fig. 9C). These increases were still seen in the paclitaxel plus NT3 siRNA-treated CD1 male (Fig. 9A) and female (Fig. 9B) mice or in the paclitaxel plus tamoxifen-treated NT3 cKD male mice (Fig. 9C). Basal levels of CCL2 and TrkC in the bilateral L3/4 DRGs from the vehicle plus NT3 siRNA-treated CD1 male and female mice or from the vehicle plus tamoxifen-treated NT3 cKD male mice were not altered (Fig. 9A–C). Consistently, microinjection of AAV5-NT3, but not AAV5-GFP, into the unilateral L3/4 DRGs markedly elevated the amount of CCL2 in the ipsilateral L3/4 DRGs 8 weeks after AAV5
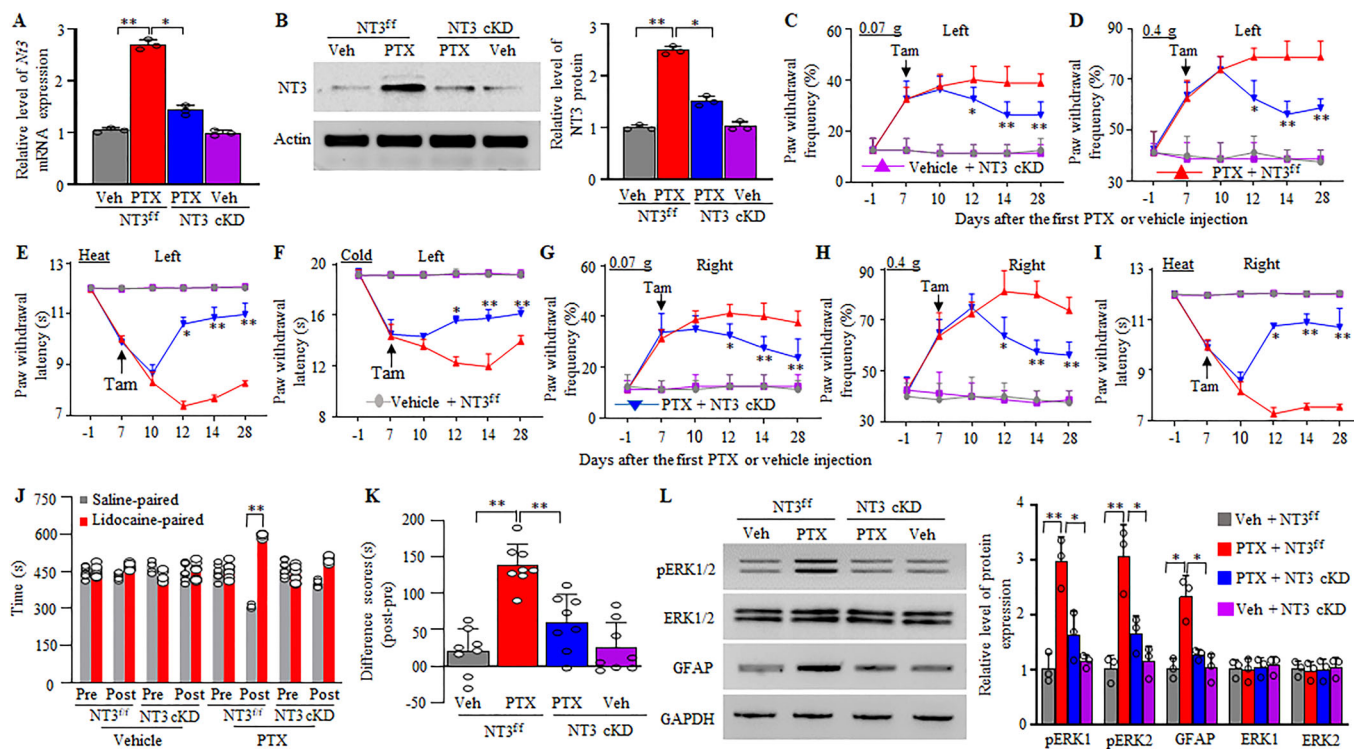
Figure 5. Effect of genetic knockdown of NT3 in DRG sensory neurons on paclitaxel-induced nociceptive hypersensitivity in male mice.
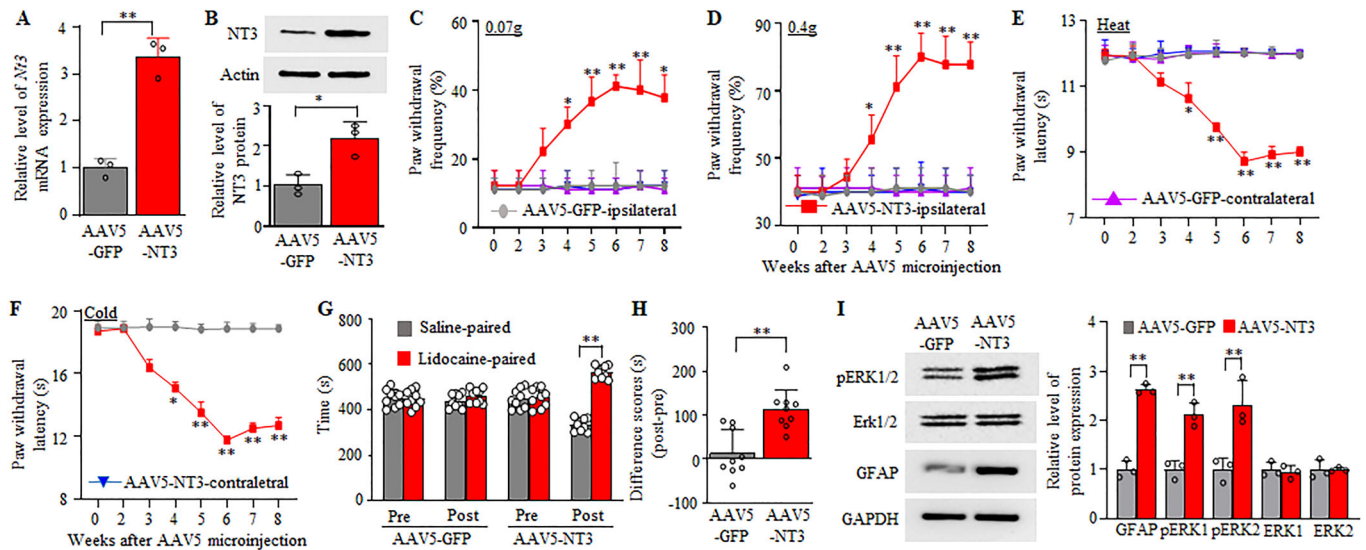
Data: mean ± SD. (A, B) Levels of *Nt3* mRNA (A) and NT3 protein (B) in the L3/4 DRGs 28 days after the first intraperitoneal (i.p.) injection of paclitaxel (PTX) or vehicle (Veh) from the tamoxifen-treated NT3^f/f mice and NT3 cKD mice. *n* = 3 biological repeated (3 mice)/group. *P < 0.05, **P < 0.01 by two-way ANOVA followed by post hoc Tukey test. (C–I) Paw withdrawal frequency to 0.07 g (C, G) and 0.4 g (D, H) von Frey filament stimuli and paw withdrawal latency to heat (E, I) and cold (F) stimuli on the left (C–F) and right (G–I) side on days as indicated from NT3^f/f mice and NT3 cKD mice with i.p. injection of tamoxifen (Tam) daily for 7 consecutive days starting at day 7 after the first i.p. injection of paclitaxel (PTX) or vehicle. *n* = 9 mice/group. *P < 0.05, **P < 0.01 versus the paclitaxel-treated NT3^f/f mice at the corresponding days by three-way ANOVA with repeated measures followed by post hoc Tukey test. (J, K) Spontaneous ongoing pain as assessed by the CPP test 21 days after the first i.p. injection of paclitaxel (PTX) or vehicle in the tamoxifen-treated NT3^f/f mice and NT3 cKD mice. Time spent in each chamber (J) and difference scores for chamber preferences calculated by subtracting preconditioning (Pre) preference time from postconditioning (Post) time spent in the lidocaine-paired chamber (K). *n* = 9 mice/group. **P < 0.01 by three-way ANOVA with repeated measures followed by post hoc Tukey test (J) or by two-way ANOVA followed by Tukey post hoc test (K). (L) Levels of p-ERK1/2, total ERK1/2 and GFAP in the L3/4 dorsal horn 28 days after the first i.p. injection of paclitaxel (PTX) or vehicle in the tamoxifen-treated NT3^f/f mice and NT3 cKD mice. *n* = 3 mice/group. *P < 0.05, **P < 0.01 by two-way ANOVA followed by post hoc Tukey test. Source data are available online for this figure.

microinjection in control scrambled siRNA-treated mice (Fig. 9D). This elevation was prevented in the AAV5-NT3 plus TrkC siRNA-treated mice, although DRG microinjection of TrkC siRNA did not change basal level of CCL2 in the AAV5-GFP-microinjectd mice (Fig. 9D). To further confirm our in vivo observations above, we explored the paclitaxel onto the cultured DRG neurons. The levels of *Nt3* mRNA, *Ccl2* mRNA, and their corresponding coding proteins were markedly increased in the paclitaxel plus negative control scrambled siRNA-treated DRG neurons (Fig. 9E,F). These increases were noticeably diminished in the paclitaxel plus NT3 siRNA-treated DRG neurons (Fig. 9E,F). NT3 siRNA did not alter basal levels of *Nt3* mRNA, *Ccl2* mRNA and their corresponding coding proteins in the vehicle-treated DRG neurons (Fig. 9E,F). Similar observations were seen in human neuroblastoma cell lines exposed to the paclitaxel or vehicle and treated with NT3 siRNA or negative control scrambled siRNA (Fig. 9G,H). In addition, the transduction of AAV5-NT3, but not AAV5-GFP, into the cultured DRG neurons dramatically increased the levels of not only *Nt3* mRNA and NT3 protein but also *Ccl2* mRNA and CCL2 protein in the negative control scrambled siRNA-treated DRG neurons

(Fig. 9I,J). NT3 siRNA treatment obviously blocked these increases in the AAV5-NT3-transducted DRG neurons (Fig. 9I,J). Single-cell RT-PCR assay showed that *Nt3* mRNA co-expressed with *TrkC* mRNA and *Ccl2* mRNA in some individual large, medium, and small DRG neurons (Fig. 10A–C). Our findings suggest that upregulated NT3 participates in paclitaxel-induced CINP at least in part due to the TrkC-mediated activation of *Ccl2* gene expression in DRG neurons.

Discussion

Systemic injection of paclitaxel produces nociceptive hypersensitivities in mice, mimicking CINP caused by chemotherapy drugs in clinical settings. Due to the limited analgesic efficacy in CINP treatments, understanding how paclitaxel injection leads to nociceptive hypersensitivity may open new avenues for managing this disorder. The present study showed the time-dependent upregulation of NT3 in DRG neurons after systemic paclitaxel injection. Preventing this upregulation blocked the paclitaxel-induced

Figure 6.   Effect of DRG NT3 overexpression on nociceptive thresholds in naive male mice.

Data: mean ± SD. (A, B) Levels of *Nt3* mRNA (A) and NT3 protein (B) in the ipsilateral L3/4 DRGs 8 weeks after microinjection of AAV5-NT3 or control AAV5-GFP in male mice. $n = 3$ biological repeats (6 mice)/group. **$P < 0.01$ by two-tailed unpaired Student t test. (C–F) Paw withdrawal frequency to 0.07 g (C) and 0.4 g (D) von Frey filament stimuli and paw withdrawal latency to heat (E) and cold (F) stimuli on the ipsilateral and contralateral sides on weeks as indicated after microinjection of AAV5-NT3 or AAV5-GFP into unilateral L3/4 DRGs. $n = 9$ mice/group. *$P < 0.05$, **$P < 0.01$ versus the AAV5-GFP group on the ipsilateral side at the corresponding time points by three-way ANOVA with repeated measures followed by Tukey post hoc test. (G, H) Spontaneous ongoing pain as assessed by the CPP test 8 weeks after microinjection of AAV5-NT3 or AAV5-GFP into unilateral L3/4 DRGs. Time spent in each chamber (G) and difference scores for chamber preferences calculated by subtracting preconditioning (Pre) preference time from postconditioning (Post) time spent in the lidocaine-paired chamber (H). $n = 9$ mice/group. **$P < 0.01$ by two-way ANOVA with repeated measures followed by post hoc Tukey test (G) or by two-tailed unpaired Student t test (H). (I) Levels of p-ERK1/2, total ERK1/2 and GFAP in the ipsilateral L3/4 dorsal horn 8 weeks after microinjection of AAV5-NT3 or AAV5-GFP into unilateral L3/4 DRGs. $n = 3$ mice/group. **$P < 0.01$ by two-tailed unpaired Student t test. Source data are available online for this figure.

increase in DRG CCL2 expression and nociceptive hypersensitivity. Mimicking this upregulation elevated TrkC-mediated DRG CCL2 expression and enhanced TrkC-mediated responses to mechanical, heat, and cold stimuli in mice without paclitaxel injection. Given that *Nt3* mRNA co-expressed with *TrkC* mRNA and *Ccl2* mRNA in individual DRG neurons, our findings suggest that NT3 contributes to CINP likely through TrkC-mediated activation of *Ccl2* gene in the DRG.

NT3, like two other neurotrophins brain-derived neurotrophic factor (Huang et al, 2021) and nerve growth factor (Nakahashi et al, 2014), can be upregulated in injured DRG under neuropathic pain conditions. Peripheral nerve injury increased NT3 and TrkC expression in the ipsilateral DRG neurons (Kazemi et al, 2017; Tender et al, 2011; Wang et al, 2008). NT3 and TrkC were also increased in the DRG, sciatic nerve, and skin nerves under the conditions of rat and human diabetic neuropathy (Cai et al, 1999; Kennedy et al, 1998; Shimoshige et al, 2010; Terenghi et al, 1997). However, two early studies reported the decreases of *Nt3* mRNA, *TrkC* mRNA and NT3 protein in skeletal muscles, DRG, or sciatic nerve of streptozotocin (STZ)-treated rats (Fernyhough et al, 1998; Ihara et al, 1996). The opposing data from these two studies might be related to performing insensitive and non-quantitative Northern blotting and ELSA assays and tissue collection at the late stage (12–14 w) of STZ rats (at this stage, peripheral nerves are degraded), as one of these two studies showed an increasing tendency of DRG *TrkC* mRNA 6 weeks post-STZ (Fernyhough et al, 1998). In the present study, we demonstrated that systemic paclitaxel injection time-dependently upregulated the expression of

Nt3 mRNA and NT3 protein in the DRG, but not in spinal cord. The latter may be related the fact that paclitaxel cannot penetrate through the blood-brain barrier. Interestingly, an earlier increase in NT3 protein rather than *Nt3* mRNA in the DRG on day 7 after the first paclitaxel injection was unexpectedly observed. The reason of how this occurs is unclear, but it appears that paclitaxel injection may have more strongly promoted effect on NT3 protein translation and posttranslational modification than on *Nt3* mRNA transcription and post-transcriptional modification in the DRG at the early time. This upregulation is correlated with paclitaxel-induced nociceptive hypersensitivity. Because commercially available NT3 antibodies do not apply for immunohistochemistry staining, we conducted ISHH assay for detecting *Nt3* mRNA cellular distribution. We found that paclitaxel-induced *Nt3* mRNA upregulation occurred exclusively in small, medium, and large DRG neurons. These findings suggest that upregulated NT3 in the DRG neurons may be implicated in the paclitaxel-induced CINP. Our findings also indicate that *Nt3* gene is transcriptionally activated under the conditions of paclitaxel exposure. Although the detailed mechanisms underlying this activation are still elusive in the present study, the possible involvement of transcription factors, epigenetic modifications and/or increase in RNA stability in paclitaxel-induced DRG *Nt3* mRNA upregulation cannot be ruled out, and further investigation is needed in our going research.

In this study, we employed both NT3 siRNA and sensory neuron-specific inducible NT3 cKD transgenic mice to examine the role of DRG NT3 in the paclitaxel-induced CINP. We demonstrated that either the microinjection of NT3 siRNA into the
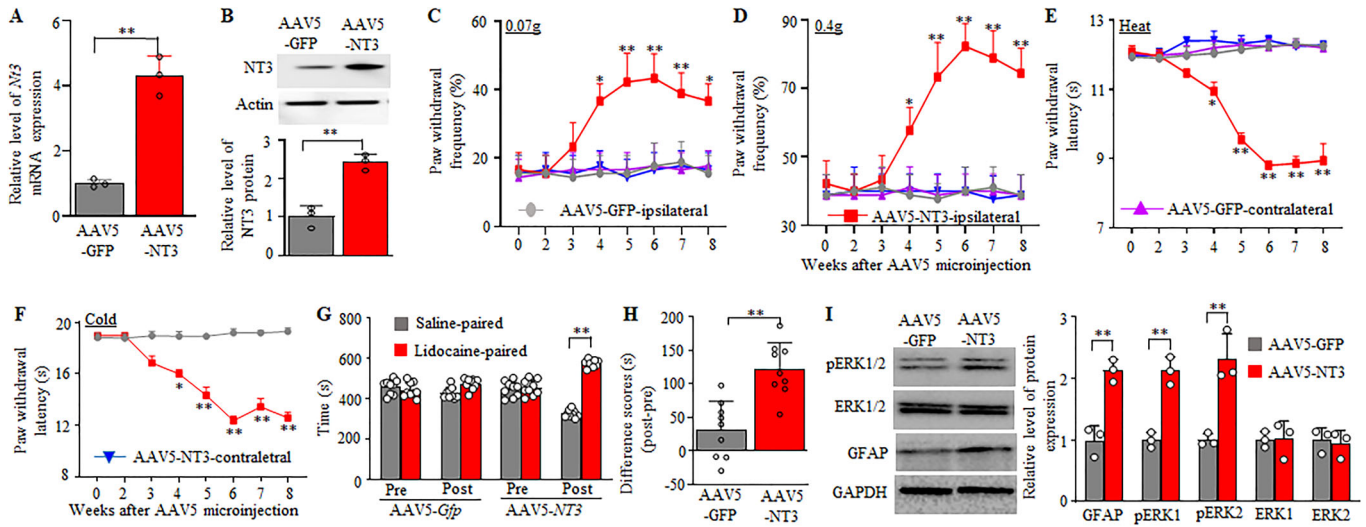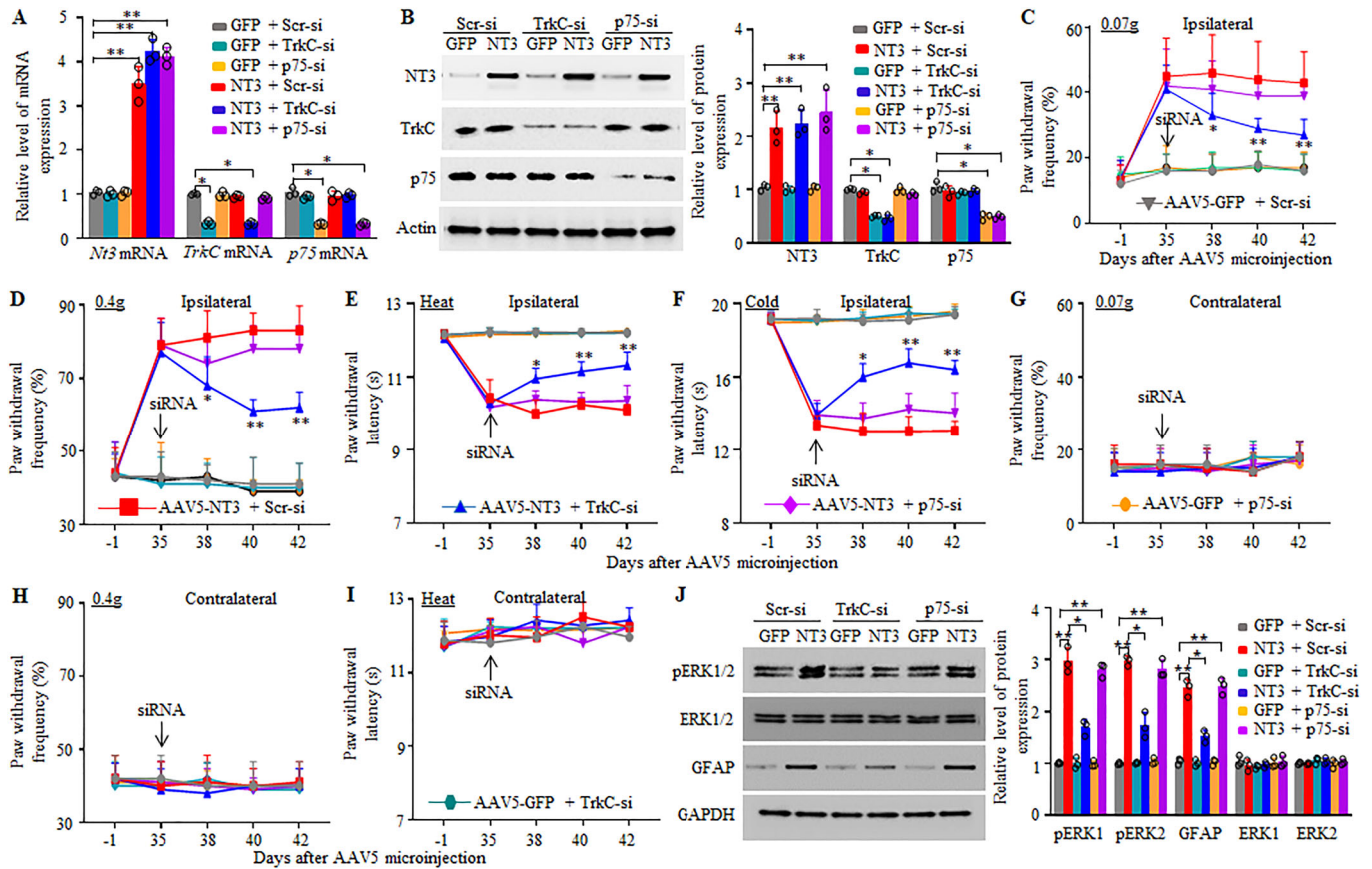
Figure 7. Effect of DRG NT3 overexpression on nociceptive thresholds in naive female mice.

Data: mean ± SD. (**A, B**) Levels of *Nt3* mRNA (**A**) and NT3 protein (**B**) in the ipsilateral L3/4 DRGs 8 weeks after microinjection of AAV5-NT3 or control AAV5-GFP in female mice. $n = 3$ biological repeats (6 mice)/group. **$P < 0.01$ by two-tailed unpaired Student t test. (**C–F**) Paw withdrawal frequency to 0.07 g (**C**) and 0.4 g (**D**) von Frey filament stimuli and paw withdrawal latency to heat (**E**) and cold (**F**) stimuli on the ipsilateral and contralateral sides on weeks as indicated after microinjection of AAV5-NT3 or AAV5-GFP into unilateral L3/4 DRGs. $n = 9$ mice/group. *$P < 0.05$, **$P < 0.01$ versus the AAV5-GFP group on the ipsilateral side at the corresponding time points by three-way ANOVA with repeated measures followed by the Tukey post hoc test. (**G, H**) Spontaneous ongoing pain as assessed by the CPP test 8 weeks after microinjection of AAV5-NT3 or AAV5-GFP into unilateral L3/4 DRGs. Time spent in each chamber (**G**) and difference scores for chamber preferences calculated by subtracting preconditioning (Pre) preference time from postconditioning (Post) time spent in the lidocaine-paired chamber (**H**). $n = 9$ mice/group. **$P < 0.01$ by two-way ANOVA with repeated measures followed by post hoc Tukey test (**G**) or by two-tailed unpaired Student t test (**H**). (**I**) Levels of p-ERK1/2, total ERK1/2 and GFAP in the ipsilateral L3/4 dorsal horn 8 weeks after microinjection of AAV5-NT3 or AAV5-GFP into unilateral L3/4 DRGs. $n = 3$ mice/group. **$P < 0.01$ by two-tailed unpaired Student t test. Source data are available online for this figure.

unilateral L3/4 DRGs or i.p. injection of tamoxifen in the NT3 cKD mice blocked the paclitaxel-induced DRG NT3 upregulation and nociceptive hypersensitivity without affecting basal (acute) pain and locomotor functions. These findings indicate the specificity and selectivity of the effects of both strategies. NT3 siRNA directly knocks down NT3 expression in the unilateral L3/4 DRGs, but siRNA may have potential off-targets and lack the cell type transfection selectivity. In contrast, tamoxifen injection-induced NT3 knockdown in NT3 cKD mice occurs exclusively in sensory neurons, although this knockdown is seen in all DRGs and trigeminal ganglions. Thus, the data from these two strategies complement each other. Unexpectedly, DRG microinjection of NT3 siRNA or tamoxifen injection in NT3 cKD mice failed to significantly knock down basal expression of *Nt3* mRNA and NT3 protein in the DRG from the vehicle-treated mice or in the vehicle-treated cultured DRG neurons. The reasons of why these two strategies did not affect basal NT3 expression are unclear, but it is very likely that lower basal level of NT3 expression under normal conditions cannot be markedly further knocked down by NT3 siRNA or tamoxifen at the present dosage used.

The upregulated DRG NT3 contributes to the paclitaxel-induced CINP likely through the TrkC-mediated increase of CCL2 in DRG neurons. Systemic administration of paclitaxel and oxaliplatin increased the expression of DRG CCL2 (Al-Mazidi et al, 2018; Curry et al, 2018; Illias et al, 2018; Wen et al, 2020, 2023; Zhang et al, 2016a). We also showed a robust increase in the level of CCL2 in DRGs on days 14 and 28 after the first paclitaxel injection. Pharmacological blockade or genetic knockdown of DRG CCL2

attenuated the paclitaxel-induced nociceptive hypersensitivity (Al-Mazidi et al, 2018; Curry et al, 2018; Illias et al, 2018; Zhang et al, 2016a). Increased DRG CCL2 likely is an endogenous instigator of CINP. This study demonstrated that NT3 regulated CCL2 expression via TrkC in DRG neurons after paclitaxel injection. DRG microinjection of NT3 siRNA or tamoxifen injection in NT3 cKD mice not only attenuated the paclitaxel-induced nociceptive hypersensitivity but also blocked the paclitaxel-induced increase in DRG CCL2 in both male and female mice. Conversely, DRG overexpression of NT3 increased basal expression of DRG CCL2 and led to both stimulation-dependent and independent nociceptive hypersensitivity in both male and female mice. The increase in DRG CCL2 induced by DRG NT3 overexpression could be inhibited by DRG TrkC knockdown. Our in vitro experiments further revealed that CCL2 expression at both mRNA and protein levels was increased in cultured DRG neurons exposed to paclitaxel or NT3. These increases were attenuated after NT3 knockdown. Given the co-expression of *Nt3* mRNA, *TrkC* mRNA and *Ccl2* mRNA in some individual DRG neurons, the antinociception resulting from blocking the paclitaxel-induced DRG NT3 upregulation likely stems from the failure of TrkC-mediated transcriptional activation of *Ccl2* gene in DRG neurons, although the detailed mechanisms of how NT3/TrkC transcriptionally actives the promoter of *Ccl2* gene are still unknown. Silence of CCL2 protein expression reduced the excitability of DRG neurons (Jung et al, 2008; Sun et al, 2006; Van Steenwinckel et al, 2011), subsequently decreased the release of primary afferent transmitters/neuromodulators (Baba et al, 2003; Gao et al, 2009) and finally impaired spinal

Figure 8. Effect of DRG TrkC or p75 NTR knockdown on DRG NT3 overexpression-induced nociceptive hypersensitivity in naive male mice.

Data: mean ± SD. (A, B) Levels of *Nt3*, *TrkC*, and *p75 NTR* mRNAs (A) and their respective proteins (B) in the ipsilateral L3/4 DRGs 42 days after microinjection of AAV5-NT3 (NT3) or AAV5-GFP (GFP) into unilateral L3/4 DRGs of the mice with co-microinjection of control scrambled siRNA (Scr-si), TrkC siRNA (TrkC-si), or p75 NTR siRNA (p75-si). $n = 3$ biological repeats (6 mice)/group. *$P < 0.05$, **$P < 0.01$ by one-way ANOVA followed by post hoc Tukey test. (C–I) Paw withdrawal frequencies to 0.07 g (C, G) and 0.4 g (D, H) von Frey filament stimuli and paw withdrawal latencies to heat (E, I) and cold stimuli (F) on the ipsilateral (C–F) and contralateral (G–I) sides on days as indicated after AAV-NT3 or AAV-GFP microinjection in the mice with co-microinjection of control scrambled siRNA (Scr-si), TrkC siRNA (TrkC-si), or p75 NTR siRNA (p75-si) starting at 35 days after AAV5 microinjection. $n = 9$ mice/group. *$P < 0.05$, **$P < 0.01$ versus the AAV5-NT3 plus control scrambled siRNA-treated group at the corresponding days by two-way ANOVA with repeated measures followed by Tukey post hoc test. (J) Levels of p-ERK1/2, total ERK1/2 and GFAP in the ipsilateral L3/4 dorsal horn on day 42 after microinjection of AAV5-NT3 (NT3) or AAV5-GFP (GFP) into unilateral L3/4 DRGs of the mice with co-microinjection of control scrambled siRNA (Scr-si), TrkC siRNA (TrkC-si), or p75 NTR siRNA (p75-si). $n = 3$ mice/group. *$P < 0.05$, **$P < 0.01$ by one-way ANOVA followed by Tukey post hoc test. Source data are available online for this figure.

cord central sensitization formation. Indeed, we found that blocking DRG NT3 upregulation reduced the paclitaxel-induced hyperactivation in dorsal horn astrocytes and neurons. Our findings on the role of DRG NT3 in the paclitaxel-induced CINP are consistent with NT3 functions in nerve trauma-induced neuropathic pain in most previous studies (Deng et al, 2000; Quintao et al, 2008; White, 1998, 2000; Zhou et al, 2000).

In conclusion, we have explored a novel mechanism by which upregulated NT3 increased the TrkC-mediated expression of CCL2 in DRG neurons under the conditions of paclitaxel-induced CINP. Since blocking the upregulated DRG NT3 alleviated paclitaxel-induced CINP without altering basal or acute pain or locomotor functions, NT3 may be a potential target for treating this disorder. In particular, NT3 knockdown blocked the paclitaxel-induced CCL2 expression in in vitro human neuroblastoma cell lines. This suggests that targeting NT3 has strong potential for translation in clinical CINP management. Nevertheless, it should be noted that

NT3 is expressed in other body tissues in addition to the DRG, and potential side effects caused by targeting NT3 should be considered.

Methods

Animal preparations

Adult male and female CD1 mice (2–3 months) weighing between 25 and 30 g were purchased from Charles River Laboratory (Wilmington, MA). The NT3[f/f] mice and Advillin[Cre-ERT2/+] mice (background: C57/BL6) were purchased from Jackson Laboratory (Bar Harbor, ME). To obtain the sensory neuron-specific inducible conditional NT3 knockdown (NT3 cKD) mice, we crossbred male Advillin[Cre-ERT2/+] mice with female NT3[f/f] mice. All mice were housed in the central housing facility at Rutgers New Jersey Medical School under a standard 12-h light/dark cycle, with water and food pellets available ad libitum. The
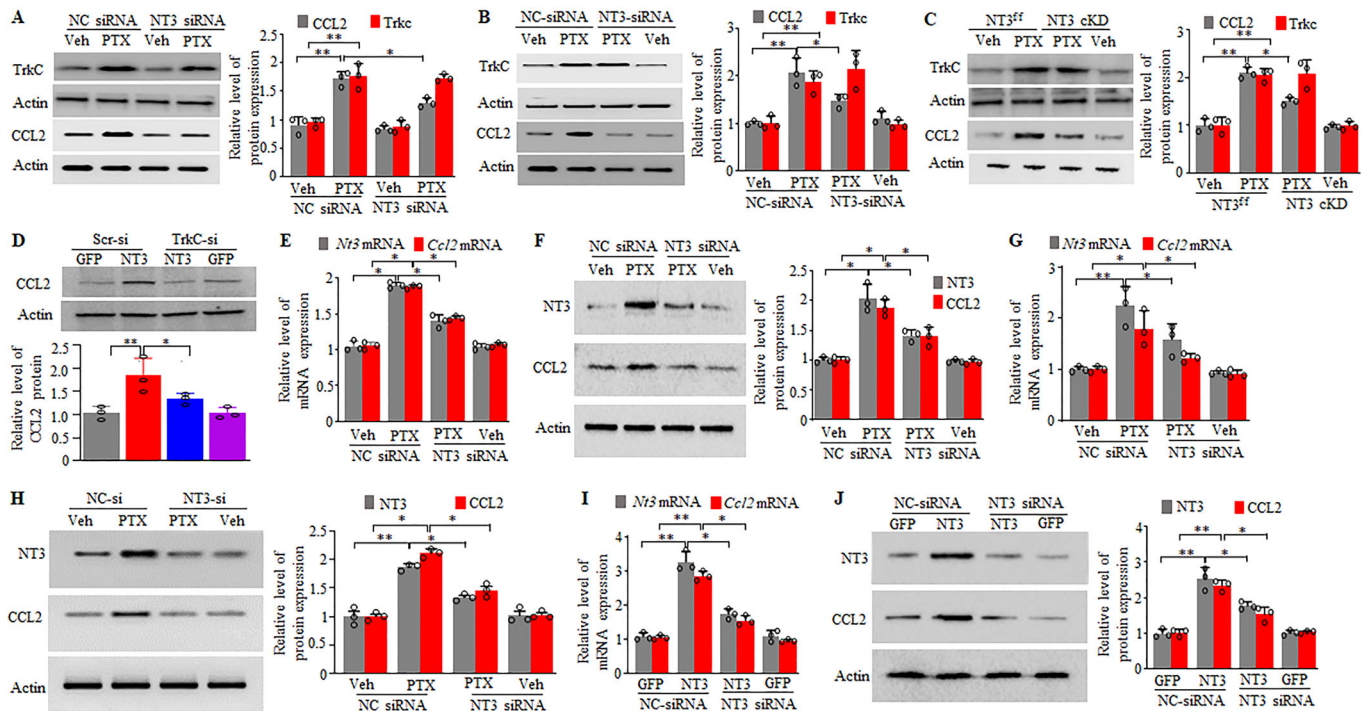
Figure 9. Role of upregulated DRG NT3 in paclitaxel-induced CCL2 expression in DRG.

Data: mean ± SD. Data: mean ± SD. (A–C) Levels of CCL2 and TrkC proteins in the ipsilateral L3/4 DRGs 14 days after the first injection of paclitaxel (PTX) or vehicle (Veh) from the NT3 siRNA- or negative control scrambled siRNA (NC siRNA)-microinjected male (A) and female (B) mice or 28 days after the first injection of paclitaxel or vehicle from the tamoxifen-treated NT3$^{f/f}$ mice and NT3 cKD mice (C). $n = 3$ biological repeats (6 mice in A and B and 3 mice in C)/group. *$P < 0.05$, **$P < 0.01$ by two-way ANOVA followed by post hoc Tukey test. (D) Level of CCL2 protein in the ipsilateral L3/4 DRGs 42 days after microinjection of AAV5-NT3 (NT3) or AAV5-GFP (GFP) into unilateral L3/4 DRGs of the mice with co-microinjection of control scrambled siRNA (Scr-si), or TrkC siRNA (TrkC-si). $n = 3$ biological repeats (6 mice)/group. *$P < 0.05$, **$P < 0.01$ by one-way ANOVA followed by post hoc Tukey test. (E–H) Levels of $Nt3$ mRNA (E, G), $Ccl2$ mRNA (E, G) and their respective proteins (F, H) in the cultured DRG neurons (E–F) or in human neuroblastoma cell lines (G, H) with transfection of NT3 siRNA or negative control scrambled siRNA (NC siRNA) plus with exposure to paclitaxel (PTX) or vehicle (Veh). $n = 3$ biological repeats. *$P < 0.05$, **$P < 0.01$ by one-way ANOVA followed by post hoc Tukey test. (I, J) Levels of $Nt3$ mRNA (I), $Ccl2$ mRNA (I) and their respective proteins (J) in the cultured DRG neurons with transduction of AAV5-NT3 (NT3) or AAV5-GFP (GFP) plus with transfection of NT3 siRNA or negative control scrambled siRNA (NC siRNA). $n = 3$ biological repeats. *$P < 0.05$, **$P < 0.01$ by one-way ANOVA followed by post hoc Tukey test. Source data are available online for this figure.

Animal Care and Use Committee at Rutgers New Jersey Medical School approved all experimental procedures (Protocol number: PROTO201702655), which were also consistent with the ethical guidelines of the US National Institutes of Health and the International Association for the Study of Pain. The animals were randomly assigned into different groups. The experimenters were blinded to all treated conditions. All efforts were made to minimize mouse suffering and to reduce the number of mice used.

Paclitaxel CINP mouse model

The mouse model of paclitaxel CINP was conducted as described previously (Jia et al, 2022; Mao et al, 2019; Wei et al, 2021; Wen et al, 2023; Yang et al, 2021). Briefly, paclitaxel (6 mg/ml in 50% Cremophor El (Sigma-Aldrich, St. Louis, MO) and 50% ethanol (Sigma-Aldrich)) was diluted in sterile saline to a final concentration of 0.4 mg/ml and administered intraperitoneally at a dose of 4 mg/kg every other day for 8 consecutive days. The vehicle was prepared as the same as the preparation described above without paclitaxel.

DRG microinjection

DRG microinjection was conducted as described with minor modification (Jia et al, 2022; Mao et al, 2019; Wei et al, 2021; Wen et al, 2023; Yang et al, 2021). After the mouse was anesthetized with isoflurane, a dorsal midline incision was made in the lower lumbar back region. The unilateral L4 and/or L3 articular processes were exposed and then removed. Viral solution (1 µl/DRG; 4–9 × 10^{12} VG/ml; dissolved in PBS) or siRNA solution (1 µl/DRG; 40–80 µM; Santa Cruz Biotechnology (catalog number: sc-42126 for NT3 siRNA)) was injected into ipsilateral exposed L4 or L3/4 DRGs with the use of a glass micropipette connected to a Hamilton syringe. siRNA was dissolved in TurboFect in vivo transfection reagent (Thermo Scientific Inc, Pittsburgh, PA) to improve delivery and prevent degradation of siRNA (Li et al, 2017b). After injection, the 10-min pipette retention was used before it was removed. The surgical field was irrigated with sterile saline, and the skin incision closed with wound clips. None of the microinjected mice showed signs of paresis or other abnormalities.
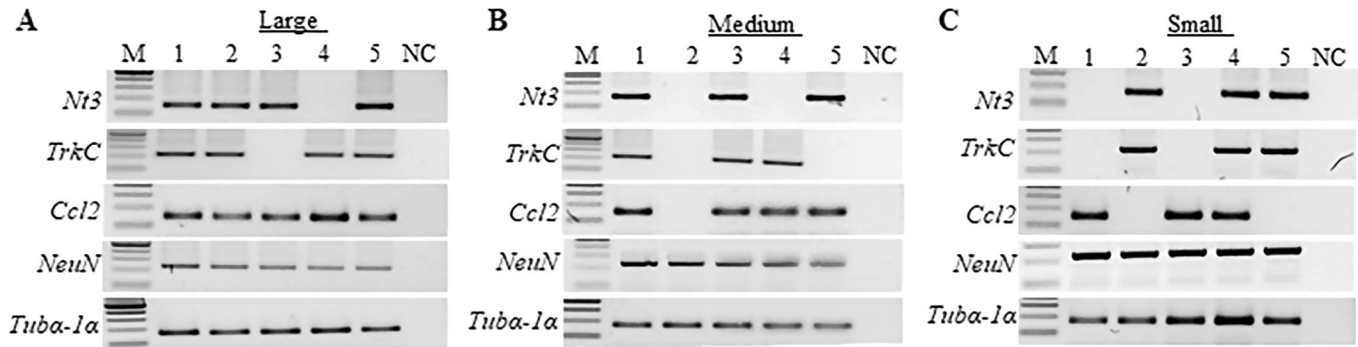
Figure 10. *Nt3* mRNA, *TrkC* mRNA and *Ccl2* mRNA co-exists in individual small, medium and large DRG neurons.

Co-expression analysis of *Nt3* mRNA, *TrkC* mRNA and *Ccl2* mRNA in individual large (>35 μm in diameter; **A**), medium (25–35 μm in diameter; **B**), and small (<25 μm in diameter; **C**) DRG neurons from naive mice ($n = 2$) by single-cell RT-PCR assay. *NeuN* mRNA is used as a neuronal marker. *Tuba-1α* mRNA is used as a loading control. M DNA ladder marker, NC no cDNA. $n = 5$ neurons/size. Source data are available online for this figure.

Behavioral testing

The evoked behavioral testing, including mechanical, heat, and cold tests, was carried out in sequential order at 1-h intervals. Conditional place preference (CPP) testing was performed 6 weeks after microinjection. Locomotor function testing was carried out before the tissue collection.

Paw withdrawal thresholds in response to mechanical stimulation were measured with two calibrated von Frey filaments (0.07 and/or 0.4 g, Stoelting Co., Wood Dale, IL) as described (Jia et al, 2022; Mao et al, 2019; Wei et al, 2021; Wen et al, 2023; Yang et al, 2021). Briefly, mice were placed in a Plexiglas chamber on an elevated mesh screen. Each von Frey filament was applied to the plantar sides of both hind paws 10 times. A quick withdrawal of the paw was regarded as a positive response. The number of positive responses among 10 applications was recorded as percentage withdrawal frequency [number of paw withdrawals/10 trials) × 100 = % response frequency].

Paw withdrawal latencies in response to noxious heat stimulation were examined as published (Jia et al, 2022; Mao et al, 2019; Wei et al, 2021; Wen et al, 2023; Yang et al, 2021). Briefly, mice were placed in a Plexiglas chamber on a glass plate. A beam of light emitted from a hole in the light box of a Model 336 Analgesia Meter (IITC Inc. Life Science Instruments. Woodland Hills, CA) was applied to the middle of the plantar surface of each hind paw. A quick lift of the hind paw was regarded as a signal to turn off the light. The length of time between the start and the stop of the light beam was defined as the paw withdrawal latency. For each side, three trials at 5-min intervals were carried out. A cutoff time of 20 s was used to avoid tissue damage to the hind paw.

Paw withdrawal latencies to noxious cold (0 °C) were observed as described (Jia et al, 2022; Mao et al, 2019; Wei et al, 2021; Wen et al, 2023; Yang et al, 2021). Mice were placed in a Plexiglas chamber on the cold aluminum plate, the temperature of which was monitored continuously by a thermometer. The paw withdrawal latency was recorded as the length of time between placement and the first sign of the mouse jumping and/or flinching. Each trial was repeated three times at 10-min intervals on the ipsilateral side. To avoid tissue damage, a cutoff time of 20 s was used.

CPP test was carried out as described with minor modifications (Jia et al, 2022; Mao et al, 2019; Wei et al, 2021; Wen et al, 2023; Yang et al, 2021). Briefly, an apparatus with two Plexiglas chambers connected with an internal door (Med Associates Inc., St. Albans, VT) was used. One of the chambers was made of a rough floor and walls with black and white horizontal stripes, and another one was composed of a smooth floor and walls with black and white vertical stripes. The movement of the mice and time spent in each chamber were monitored by photobeam detectors installed along the chamber walls and automatically recorded in MED-PC IV CPP software. Mice were first preconditioned for 30 min with full access to two chambers to habituate them to the environment. At the end of the preconditioning phase, basal duration spent in each chamber was recorded within 15 min to check whether animals had a preexisting chamber bias. Mice spending more than 80% or less than 20% of total time in any chamber were excluded from further testing. The conditioning protocol was performed for the following 3 days with the internal door closed. The mice first received an intrathecal injection of saline (5 μl) specifically paired with one conditioning chamber in the morning. Six hours later, lidocaine (0.8% in 5 μl of saline) was given intrathecally paired with the opposite conditioning chamber in the afternoon. Lidocaine at this dosage did not affect motor function. The injection order of saline and lidocaine was switched every day. On the test day, at least 20 h after the conditioning, the mice were placed in one chamber with free access to both chambers. The duration of time that each mouse spent in each chamber was recorded for 15 min. Score differences were calculated as test time-preconditioning time spent in the lidocaine chamber.

Locomotor function was examined as described (Jia et al, 2022; Mao et al, 2019; Wei et al, 2021; Wen et al, 2023; Yang et al, 2021). Three reflexes were conducted as follows. For the placing reflex, the placed positions of the hind limbs were slightly lower than those of the forelimbs, and the dorsal surfaces of the hind paws were brought into contact with the edge of a table. Whether the hind paws were placed on the table surface reflexively was recorded. For the grasping reflex, after the mouse was placed on a wire grid, whether the hind paws grasped the wire on contact was recorded. For the righting reflex, when the mice were placed on its back on a flat surface, whether it immediately assumed the normal upright

position was recorded. Each trial was repeated 5 times at 5-min intervals and the scores for each reflex were recorded based on counts of each normal reflex.

Cell culture and transfection

Human neuroblastoma cell line (SK-N-BE(2)-C; ATCC, Manassas, VA) cultures and DRG neuronal cultures were prepared as previously described (Jia et al, 2022; Mao et al, 2019; Wei et al, 2021; Wen et al, 2023; Yang et al, 2021). Briefly, SK-N-BE(2)-C cells were cultured in Minimum Essential medium/NEAA: F-12 (Gibco/Thermo Fisher Scientific) containing 20% fetal bovine serum (FBS), w/o L-glutamine (200 mM) (Gibco/Thermo Fisher Scientific), and 100 units/ml Penicillin and 100 μg/ml Streptomycin (Quality Biological, Gaithersburg, MD). For primary DRG neuronal cultures, after CD1 male mice (≥4 weeks) were euthanized with isoflurane, all DRGs were collected in cold Neurobasal Medium (Gibco/Thermo Fisher Scientific) containing 10% fetal bovine serum (JR Scientific, Woodland, CA), 5 mL L-glutamine (200 mM) (Gibco/Thermo Fisher Scientific), 10 mL B-27® Supplement (50×) (Gibco/Thermo Fisher Scientific), 100 units/ml penicillin and 100 μg/ml streptomycin (Quality Biological, Gaithersburg, MD). The DRGs were then treated with enzyme solution (5 mg/ml dispase, 1 mg/ml collagenase type I) in Hanks' balanced salt solution (HBSS) without Ca^{2+} and Mg^{2+} (Gibco/Thermo Fisher Scientific). After trituration and centrifugation, dissociated cells were resuspended in mixed Neurobasal Medium and plated in a six-well plate coated with 50 μg/ml poly-D-lysine (Sigma, St. Louis, MO) at $1.5–4 \times 10^5$ cells. The cell lines or DRG neurons were incubated at 5% CO_2 and 37 °C. On the second day, 4–10 μl of virus $(6–9 \times 10^{12}$ tu/μl), 1 μmol of paclitaxel or 100 nM of siRNA (transfected with Lipofectamine 2000) was added to each 2 ml well. The cells were collected 3 days later.

In situ hybridization histochemistry and co-immunohistochemistry

Mice were deeply anesthetized with isoflurane and transcardially perfused with 25–30 ml of 0.1 M phosphate-buffered saline (PBS, pH 7.4) followed by 30–50 ml of 4% paraformaldehyde in 0.1 M PBS. Following perfusion, DRG was harvested, post-fixed for 4–6 h at 4 °C in the same fixative solution, and cryoprotected in 30% sucrose overnight. In total, 20-μm transverse sections were cut on a cryostat. Every third section was collected from each DRG. In situ hybridization histochemistry (ISHH) was carried out by using a protocol tailored to the IsHyb In Situ Hybridization (ISH) Kit (K2191050; Miramar Beach, FL) with minor modification (Pan et al, 2021). The probe specifically for Nt3 mRNA was prepared by in vitro transcription and labeled with digoxigenin-dUTP according to the manufacturer's instructions (Roche Diagnostics, Indianapolis, IN). After being treated with proteinase K and pre-hybridized, the sections were hybridized with digoxigenin-dUTP-labeled Nt3 probes for over two nights at 62 °C. After being blocked for 1 h at RT in 0.01 M PBS/0.3% Triton X-100 containing 4% goat serum, the sections were incubated with AP-conjugated anti-digoxigenin antibody plus chicken anti-β-tubulin III (1:200, catalog number: MAB5564; EMD Millipore; Danvers, MA), rabbit anti-glutamine synthetase (1:500, catalog number: G2781; Sigma-Aldrich; St. Louis, MO), mouse anti-calcitonin gene-related peptide

(CGRP, 1:50; catalog number: ab283568; Abcam), rabbit anti-NF200 (1:100, catalog number: N4142; Sigma-Aldrich), biotinylated IB4 (1:100, catalog number: L2140; Sigma-Aldrich) or mouse anti-TH (1:200, catalog number: sc-25269; Santa Cruz; Dallas, TX) at overnight at 4 °C. After being washed, the sections were incubated with avidin labeled with FITC (1:200, Sigma-Aldrich) or goat anti-rabbit antibody, anti-chicken antibody or anti-mouse antibody conjugated with Cy2 (1:200, Jackson ImmunoReseach Labs; West Grove, PA) at room temperature for 1 h. The fluorescent signals were developed with Fast Red. The immuno-fluorescent images were captured under a Leica DMI4000 fluorescence microscope (Leica) with a DFC365 FX camera (Leica). The number of the neurons (with nucleus) double-labeled by Nt3 mRNA and each marker and the number of the neurons (with nucleus) single labeled by each marker in each section were counted. At least 3–4 sections per DRG were examined. The average percentage of Nt3 mRNA-positive neurons per section within each marker was calculated.

Western blotting assay

Protein extraction and Western blotting were carried out according to our published protocols (Jia et al, 2022; Mao et al, 2019; Wei et al, 2021; Wen et al, 2023; Yang et al, 2021). Briefly, four DRGs were pooled to obtain enough protein. DRGs or spinal cord were homogenized and the cultured cells ultrasonicated on ice with the lysis buffer (10 mM Tris, 1 mM phenylmethylsulfonyl fluoride, 5 mM $MgCl_2$, 5 mM EGTA, 1 mM EDTA, 1 mM DTT, 40 μM leupeptin, 250 mM sucrose). After the homogenates were centrifugated at $1000 \times g$ for 15 min at 4 °C, the supernatant (membrane/cytosolic fractions) was collected. The protein concentrations were measured using the Bio-Rad protein assay (Bio-Rad). Twenty μg per sample were loaded onto a 4–15% stacking/7.5% separating SDS-polyacrylamide gel (Bio-Rad Laboratories, Hercules, CA). The protein was then electrophoretically transferred onto a polyvinylidene difluoride membrane (Bio-Rad Laboratories). After the membrane was first incubated in the blocking buffer (5% nonfat milk plus 0.1% Tween-20 in the Tris-buffered saline) for 1 h at room temperature, they were incubated with primary antibodies at 4 °C overnight or two nights. The primary antibodies included rabbit anti-NT3 (1:250; Alomone Labs, catalog number: ANT-003; Jerusalem, Isreael), rabbit anti-MCP-1 (1:1000, catalog number: ab315478; Abcam; Waltham, MA), rabbit anti-p75NTR (1:1000, catalog number: 07-476; Sigma-Aldrich), rabbit anti-TrkC (1:400, catalog number: ANT-020; Alomone), rabbit anti-ERK1/2 (1:1000, catalog number: 4370S; Cell Signaling Technology), rabbit anti-phosphorylated ERK1/2 (p-ERK1/2; 1:1000; catalog number: 3670S; Cell Signaling Technology), mouse anti-GFAP (1:1000, catalog number: 3670S; Cell Signaling Technology), rabbit anti-GAPDH (1:1000, catalog number: G9545; Sigma-Aldrich) and mouse anti-actin (1:1000, catalog number: sc-47778; Santa Cruz). The proteins were detected by horseradish peroxidase-conjugated anti-rabbit and anti-mouse secondary antibodies (1:5000, Jackson ImmunoResearch) at room temperature for 1 h and visualized by western peroxide reagent and luminol/enhancer reagent (Clarity Western ECL Substrate, Bio-Rad) using ChemiDoc XRS System with Image Lab software (Bio-Rad). The intensity of the band was quantified with densitometry using Image J software. All bands were normalized to actin or GAPDH.

Quantitative real-time RT-PCR assay

RNA extraction and quantitative real-time RT-PCR assay were carried out according to our published protocol (Jia et al, 2022; Mao et al, 2019; Wei et al, 2021; Wen et al, 2023; Yang et al, 2021). Briefly, four DRGs were pooled to obtain enough protein. Total RNA was extracted from the DRG by using TRIzol-chloroform methods (Invitrogen), treated with an overdose of deoxyribonuclease I (New England Biolabs), and reverse-transcribed with the ThermoScript Reverse Transcriptase (Invitrogen/Thermo Fisher Scientific) and oligo(dT) primers (Invitrogen/Thermo Fisher Scientific). The template (4 μl) was amplified in a Bio-Rad CFX96 real-time PCR system by using the primers for $Nt3$, $Ccl2$ or $Tuba1a$ mRNAs (Table EV2). Each sample was repeated three times with a 20-μl reaction volume containing 200 nM forward and reverse primers, 10 μl of SsoAdvanced Universal SYBR Green Supermix (Bio-Rad Laboratories), and 20 ng of cDNA. The PCR amplification included 30 s at 95 °C, 30 s at 60 °C, 30 s at 72 °C, and 5 min at 72 °C for 39 cycles. All PCR data were normalized to an internal control $Tuba1a$. The ratios of mRNA levels were calculated using the ΔCt method ($2 - \Delta\Delta Ct$).

Single-cell RT-PCR assay

The freshly cultured DRG neurons from adult mice were prepared as described previously (Du et al, 2022; Pan et al, 2021; Wang et al, 2023). Four hours after plating, under an inverted microscope equipped with a micromanipulator and microinjector, a single living large (>35 μm), medium (25–35 μm), and small (<25 μm) DRG neurons were collected into a PCR tube containing 6–8 μl of cell lysis buffer (Signosis, Sunnyvale, CA) and centrifuged. The lysis solution was aliquoted into distinct PCR tubes for different genes. The RT-PCR procedure was carried out with the Single-Cell RT-PCR Assay Kit according to the instructions provided by the manufacturer (Signosis). The nest-PCR primers used are listed in Table EV2. The PCR products were analyzed on ethidium bromide-stained 2% agarose gels.

Plasmid construction and virus production

The full-length sequences of $Nt3$ mRNA extracted from mouse DRG were reverse-transcribed using the SuperScript IV One-Step RT-qPCR System with Platinum Taq High Fidelity Kit (Invitrogen/Thermo-Fisher Scientific) and amplified by PCR with gene-specific primers listed in the Table EV2. The resulting segment was inserted into the pro-viral plasmid at the XhoI and NotI restriction sites. The recombinant clones were verified using DNA sequencing. The resulting vectors expressed the genes under the control of the cytomegalovirus promoter. For packaging of AAV5 particles, HEK-293 cells were transfected with the pro-viral plasmid expressing $Nt3$ mRNA or Gfp using a PEI Transfection method with pHelper. Three days later, the transfected cells were collected and AAV5 particles were purified using the AAV-pro Purification Kit (Takara, Mountain View, CA). The titer was determined by AAV real-time PCR titration kit (Takara).

Statistical analysis

For in vitro experiments, the cells were evenly suspended and then randomly distributed in each tested well. For in vivo experiments, the animals were distributed into various treated groups randomly.

All data were given as means ± SD. Data distribution was assumed to be normal, but this was not formally tested. The data were statistically analyzed with two-tailed, paired/unpaired Student's t test and a one-way or two-way ANOVA. When ANOVA showed a significant difference, pairwise comparisons between means were tested by the post hoc Tukey method (SigmaStat, San Jose, CA). Significance was set at $P < 0.05$.

Data availability

This study includes no data deposited in external repositories.

Expanded view data, supplementary information, appendices are available for this paper at https://doi.org/10.1038/s44319-024-00133-6.

Peer review information

A peer review file is available at https://doi.org/10.1038/s44319-024-00133-6

References

Al-Mazidi S, Alotaibi M, Nedjadi T, Chaudhary A, Alzoghaibi M, Djouhri L (2018) Blocking of cytokines signalling attenuates evoked and spontaneous neuropathic pain behaviours in the paclitaxel rat model of chemotherapy-induced neuropathy. Eur J Pain 22:810–821

Argyriou AA, Bruna J, Marmiroli P, Cavaletti G (2012) Chemotherapy-induced peripheral neurotoxicity (CIPN): an update. Crit Rev Oncol Hematol 82:51–77

Baba H, Ji RR, Kohno T, Moore KA, Ataka T, Wakai A, Okamoto M, Woolf CJ (2003) Removal of GABAergic inhibition facilitates polysynaptic A fiber-mediated excitatory transmission to the superficial spinal dorsal horn. Mol Cell Neurosci 24:818–830

Cai F, Tomlinson DR, Fernyhough P (1999) Elevated expression of neurotrophin-3 mRNA in sensory nerve of streptozotocin-diabetic rats. Neurosci Lett 263:81–84

Curry ZA, Wilkerson JL, Bagdas D, Kyte SL, Patel N, Donvito G, Mustafa MA, Poklis JL, Niphakis MJ, Hsu KL et al (2018) Monoacylglycerol lipase inhibitors reverse paclitaxel-induced nociceptive behavior and proinflammatory markers in a mouse model of chemotherapy-induced neuropathy. J Pharm Exp Ther 366:169–183

Deng YS, Zhong JH, Zhou XF (2000) Effects of endogenous neurotrophins on sympathetic sprouting in the dorsal root ganglia and allodynia following spinal nerve injury. Exp Neurol 164:344–350

Devor M (1999) Unexplained peculiarities of the dorsal root ganglion. Pain Suppl 6:S27–S35

Du S, Wu S, Feng X, Wang B, Xia S, Liang L, Zhang L, Govindarajalu G, Bunk A, Kadakia F et al (2022) A nerve injury-specific long noncoding RNA promotes neuropathic pain by increasing Ccl2 expression. J Clin Investig 132:e153563

Fernyhough P, Diemel LT, Tomlinson DR (1998) Target tissue production and axonal transport of neurotrophin-3 are reduced in streptozotocin-diabetic rats. Diabetologia 41:300–306

Gao YJ, Zhang L, Samad OA, Suter MR, Yasuhiko K, Xu ZZ, Park JY, Lind AL, Ma Q, Ji RR (2009) JNK-induced MCP-1 production in spinal cord astrocytes contributes to central sensitization and neuropathic pain. J Neurosci 29:4096–4108

Grisold W, Cavaletti G, Windebank AJ (2012) Peripheral neuropathies from chemotherapeutics and targeted agents: diagnosis, treatment, and prevention. Neuro Oncol 14(Suppl 4):iv45–iv54

Huang L, Jin J, Chen K, You S, Zhang H, Sideris A, Norcini M, Recio-Pinto E, Wang J, Gan WB et al (2021) BDNF produced by cerebral microglia promotes cortical plasticity and pain hypersensitivity after peripheral nerve injury. PLoS Biol 19:e3001337

Ihara C, Shimatsu A, Mizuta H, Murabe H, Nakamura Y, Nakao K (1996) Decreased neurotrophin-3 expression in skeletal muscles of streptozotocin-induced diabetic rats. Neuropeptides 30:309–312

Illias AM, Gist AC, Zhang H, Kosturakis AK, Dougherty PM (2018) Chemokine CCL2 and its receptor CCR2 in the dorsal root ganglion contribute to oxaliplatin-induced mechanical hypersensitivity. Pain 159:1308–1316

Ito N, Sakai A, Miyake N, Maruyama M, Iwasaki H, Miyake K, Okada T, Sakamoto A, Suzuki H (2017) miR-15b mediates oxaliplatin-induced chronic neuropathic pain through BACE1 down-regulation. Br J Pharm 174:386–395

Jia S, Wei G, Bono J, Pan Z, Zheng B, Wang B, Adaralegbe A, Tenorio C, Bekker A, Tao YX (2022) TET1 overexpression attenuates paclitaxel-induced neuropathic pain through rescuing K(2p)1.1 expression in primary sensory neurons of male rats. Life Sci 297:120486

Jimenez-Andrade JM, Herrera MB, Ghilardi JR, Vardanyan M, Melemedjian OK, Mantyh PW (2008) Vascularization of the dorsal root ganglia and peripheral nerve of the mouse: implications for chemical-induced peripheral sensory neuropathies. Mol Pain 4:10

Jung H, Toth PT, White FA, Miller RJ (2008) Monocyte chemoattractant protein-1 functions as a neuromodulator in dorsal root ganglia neurons. J Neurochem 104:254–263

Kazemi A, Rahmati M, Eslami R, Sheibani V (2017) Activation of neurotrophins in lumbar dorsal root probably contributes to neuropathic pain after spinal nerve ligation. Iran J Basic Med Sci 20:29–35

Kennedy AJ, Wellmer A, Facer P, Saldanha G, Kopelman P, Lindsay RM, Anand P (1998) Neurotrophin-3 is increased in skin in human diabetic neuropathy. J Neurol Neurosurg Psychiatry 65:393–395

Li Y, North RY, Rhines LD, Tatsui CE, Rao G, Edwards DD, Cassidy RM, Harrison DS, Johansson CA, Zhang H et al (2018) DRG voltage-gated sodium channel 1.7 is upregulated in paclitaxel-induced neuropathy in rats and in humans with neuropathic pain. J Neurosci 38:1124–1136

Li Y, Tatsui CE, Rhines LD, North RY, Harrison DS, Cassidy RM, Johansson CA, Kosturakis AK, Edwards DD, Zhang H et al (2017a) Dorsal root ganglion neurons become hyperexcitable and increase expression of voltage-gated T-type calcium channels (Cav3.2) in paclitaxel-induced peripheral neuropathy. Pain 158:417–429

Li Y, Zhang H, Zhang H, Kosturakis AK, Jawad AB, Dougherty PM (2014) Toll-like receptor 4 signaling contributes to Paclitaxel-induced peripheral neuropathy. J Pain 15:712–725

Li Z, Mao Y, Liang L, Wu S, Yuan J, Mo K, Cai W, Mao Q, Cao J, Bekker A et al (2017b) The transcription factor C/EBPbeta in the dorsal root ganglion contributes to peripheral nerve trauma-induced nociceptive hypersensitivity. Sci Signal 10:eaam5345

Makker PG, Duffy SS, Lees JG, Perera CJ, Tonkin RS, Butovsky O, Park SB, Goldstein D, Moalem-Taylor G (2017) Characterisation of immune and neuroinflammatory changes associated with chemotherapy-induced peripheral neuropathy. PLoS ONE 12:e0170814

Mao Q, Wu S, Gu X, Du S, Mo K, Sun L, Cao J, Bekker A, Chen L, Tao YX (2019) DNMT3a-triggered downregulation of K(2p) 1.1 gene in primary sensory neurons contributes to paclitaxel-induced neuropathic pain. Int J Cancer 145:2122–2134

Mao Q, Yuan J, Ming X, Wu S, Chen L, Bekker A, Yang T, Tao YX (2017) Role of dorsal root ganglion K2p1.1 in peripheral nerve injury-induced neuropathic pain. Mol Pain 13:1744806917701135

Mendell LM, Albers KM, Davis BM (1999) Neurotrophins, nociceptors, and pain. Microsc Res Tech 45:252–261

Nakahashi Y, Kamiya Y, Funakoshi K, Miyazaki T, Uchimoto K, Tojo K, Ogawa K, Fukuoka T, Goto T (2014) Role of nerve growth factor-tyrosine kinase receptor A signaling in paclitaxel-induced peripheral neuropathy in rats. Biochem Biophys Res Commun 444:415–419

Nie B, Liu C, Bai X, Chen X, Wu S, Zhang S, Huang Z, Xie M, Xu T, Xin W et al (2018) AKAP150 involved in paclitaxel-induced neuropathic pain via inhibiting CN/NFAT2 pathway and downregulating IL-4. Brain Behav Immun 68:158–168

Pan Z, Du S, Wang K, Guo X, Mao Q, Feng X, Huang L, Wu S, Hou B, Chang YJ et al (2021) Downregulation of a dorsal root ganglion-specifically enriched long noncoding RNA is required for neuropathic pain by negatively regulating RALY-triggered Ehmt2 expression. Adv Sci 8:e2004515

Quintao NL, Santos AR, Campos MM, Calixto JB (2008) The role of neurotrophic factors in genesis and maintenance of mechanical hypernociception after brachial plexus avulsion in mice. Pain 136:125–133

Richner M, Ulrichsen M, Elmegaard SL, Dieu R, Pallesen LT, Vaegter CB (2014) Peripheral nerve injury modulates neurotrophin signaling in the peripheral and central nervous system. Mol Neurobiol 50:945–970

Salvador R, Aridgides D, PereiraPerrin M (2014) Parasite-derived neurotrophic factor/trans-sialidase of *Trypanosoma cruzi* links neurotrophic signaling to cardiac innate immune response. Infect Immun 82:3687–3696

Shimoshige Y, Enomoto R, Aoki T, Matsuoka N, Kaneko S (2010) The involvement of aldose reductase in alterations to neurotrophin receptors and neuronal cytoskeletal protein mRNA levels in the dorsal root ganglion of streptozotocin-induced diabetic rats. Biol Pharm Bull 33:67–71

Sisignano M, Angioni C, Park CK, Meyer Dos Santos S, Jordan H, Kuzikov M, Liu D, Zinn S, Hohman SW, Schreiber Y et al (2016) Targeting CYP2J to reduce paclitaxel-induced peripheral neuropathic pain. Proc Natl Acad Sci USA 113:12544–12549

Sun JH, Yang B, Donnelly DF, Ma C, LaMotte RH (2006) MCP-1 enhances excitability of nociceptive neurons in chronically compressed dorsal root ganglia. J Neurophysiol 96:2189–2199

Tender GC, Kaye AD, Li YY, Cui JG (2011) Neurotrophin-3 and tyrosine kinase C have modulatory effects on neuropathic pain in the rat dorsal root ganglia. Neurosurgery 68:1048–1055

Terenghi G, Mann D, Kopelman PG, Anand P (1997) trkA and trkC expression is increased in human diabetic skin. Neurosci Lett 228:33–36

Van Steenwinckel J, Reaux-Le Goazigo A, Pommier B, Mauborgne A, Dansereau MA, Kitabgi P, Sarret P, Pohl M, Melik Parsadaniantz S (2011) CCL2 released from neuronal synaptic vesicles in the spinal cord is a major mediator of local inflammation and pain after peripheral nerve injury. J Neurosci 31:5865–5875

Wang B, Ma L, Guo X, Du S, Feng X, Liang Y, Govindarajalu G, Wu S, Liu T, Li H et al (2023) A sensory neuron-specific long non-coding RNA reduces neuropathic pain by rescuing KCNN1 expression. Brain 146:3866–3884

Wang TH, Meng QS, Qi JG, Zhang WM, Chen J, Wu LF (2008) NT-3 expression in spared DRG and the associated spinal laminae as well as its anterograde transport in sensory neurons following removal of adjacent DRG in cats. Neurochem Res 33:1–7

Wei W, Liu W, Du S, Govindarajalu G, Irungu A, Bekker A, Tao YX (2021) A compound mitigates cancer pain and chemotherapy-induced neuropathic pain by dually targeting nNOS-PSD-95 interaction and GABA(A) receptor. Neurotherapeutics 18:2436–2448

Wen CH, Berkman T, Li X, Du S, Govindarajalu G, Zhang H, Bekker A, Davidson S, Tao YX (2023) Effect of intrathecal NIS-lncRNA antisense oligonucleotides on neuropathic pain caused by nerve trauma, chemotherapy, or diabetes mellitus. Br J Anaesth 130:202–216

Wen J, Yang Y, Wu S, Wei G, Jia S, Hannaford S, Tao YX (2020) Long noncoding RNA H19 in the injured dorsal root ganglion contributes to peripheral nerve injury-induced pain hypersensitivity. Transl Perioper Pain Med 7:176–184

White DM (1998) Contribution of neurotrophin-3 to the neuropeptide Y-induced increase in neurite outgrowth of rat dorsal root ganglion cells. Neuroscience 86:257–263

White DM (2000) Neurotrophin-3 antisense oligonucleotide attenuates nerve injury-induced Abeta-fibre sprouting. Brain Res 885:79–86

Wilson-Gerwing TD, Dmyterko MV, Zochodne DW, Johnston JM, Verge VM (2005) Neurotrophin-3 suppresses thermal hyperalgesia associated with neuropathic pain and attenuates transient receptor potential vanilloid receptor-1 expression in adult sensory neurons. J Neurosci 25:758–767

Wilson-Gerwing TD, Stucky CL, McComb GW, Verge VM (2008) Neurotrophin-3 significantly reduces sodium channel expression linked to neuropathic pain states. Exp Neurol 213:303–314

Wilson-Gerwing TD, Verge VM (2006) Neurotrophin-3 attenuates galanin expression in the chronic constriction injury model of neuropathic pain. Neuroscience 141:2075–2085

Windebank AJ, Grisold W (2008) Chemotherapy-induced neuropathy. J Peripher Nerv Syst 13:27–46

Yang Y, Wen J, Zheng B, Wu S, Mao Q, Liang L, Li Z, Bachmann T, Bekker A, Tao YX (2021) CREB participates in paclitaxel-induced neuropathic pain genesis through transcriptional activation of Dnmt3a in primary sensory neurons. Neurotherapeutics 18:586–600

Yilmaz E, Gold MS (2015) Sensory neuron subpopulation-specific dysregulation of intracellular calcium in a rat model of chemotherapy-induced peripheral neuropathy. Neuroscience 300:210–218

Zhang H, Boyette-Davis JA, Kosturakis AK, Li Y, Yoon SY, Walters ET, Dougherty PM (2013) Induction of monocyte chemoattractant protein-1 (MCP-1) and its receptor CCR2 in primary sensory neurons contributes to paclitaxel-induced peripheral neuropathy. J Pain 14:1031–1044

Zhang H, Dougherty PM (2014) Enhanced excitability of primary sensory neurons and altered gene expression of neuronal ion channels in dorsal root ganglion in paclitaxel-induced peripheral neuropathy. Anesthesiology 120:1463–1475

Zhang H, Li Y, de Carvalho-Barbosa M, Kavelaars A, Heijnen CJ, Albrecht PJ, Dougherty PM (2016a) Dorsal root ganglion infiltration by macrophages contributes to paclitaxel chemotherapy-induced peripheral neuropathy. J Pain 17:775–786

Zhang Y, Chen SR, Laumet G, Chen H, Pan HL (2016b) Nerve injury diminishes opioid analgesia through lysine methyltransferase-mediated transcriptional repression of mu-opioid receptors in primary sensory neurons. J Biol Chem 291:8475–8485

Zhou XF, Deng YS, Xian CJ, Zhong JH (2000) Neurotrophins from dorsal root ganglia trigger allodynia after spinal nerve injury in rats. Eur J Neurosci 12:100–105

Author contributions

Dilip Sharma: Conceptualization; Data curation; Formal analysis; Investigation; Methodology; Writing—original draft; Project administration. **Xiaozhou Feng**: Data curation; Formal analysis; Investigation; Visualization; Methodology. **Bing Wang**: Data curation; Formal analysis; Validation; Investigation; Visualization; Methodology. **Bushra Yasin**: Validation; Investigation; Methodology; Writing—review and editing. **Alex Bekker**: Formal analysis; Validation; Investigation; Visualization; Methodology. **Huijuan Hu**: Data curation; Formal analysis; Investigation; Visualization; Project administration. **Yuan-Xiang Tao**: Conceptualization; Resources; Data curation; Software; Formal analysis; Supervision; Funding acquisition; Validation; Investigation; Visualization; Methodology; Writing—original draft; Project administration; Writing—review and editing.

Disclosure and competing interests statement

The authors declare no competing interests.